

A pH/Temperature Cascade-Responsive Polymer Nanosystem with Controlled Drug Release for Synergistic Chemo-Photothermal Therapy

R.A. Mustafa¹, M. Ran¹, Y. Wang¹, J. Yan¹, J.M. Rosenholm¹, H. Zhang¹

¹Pharmaceutical Sciences Laboratory, Faculty of Science and Engineering, Åbo Akademi University, Turku 20520, Finland

INTRODUCTION: To optimize synergistic cancer treatment, pH-temperature responsive polymer and chemo-photo thermal therapy functions (CHT-PTT) have been compiled into a single nanocomposite. Herein, poly[(Nisopropylacrylamide)co(metha acrylic acid)] (p(NIPAM-co-MAA)) modified silica coated gold nanorods have been synthesized (AuNR@MS@DOX@p(NIPAM-co-MAA)). Upon NIR radiation, gold rod like core induce hyperthermia via generating heat. Meanwhile, the polymer layer is collapsed in response to the high temperature/low pH, which allow triggering and enhancing doxorubicin release from the mesoporous silica shell reservoir at the tumor site. The efficacy of the constructed nanocomposite has been assessed through several characterization methods. A nearly zero premature release of doxorubicin at physiological pH/temperature was observed, while effective drug release is reported at higher temperature/lower pH values. In addition, *in vitro/in vivo* studies demonstrate that more efficient cancer treatment is gained by the nanocomposite comparead with pure doxorubicin (Dox) and uncoated mesoporous silica coated goldnanorods (AuNR@MS@DOX). Thus, the synthesized nanocomposite could be a potential nanocarrier system to localize synergistic chemo-photothermal therapy.

METHODS: The fabricated nanocomposite was characterized for loading capacity, release profile, photothermal efficacy, net surface charge, surface chemical composition, and morphology using UV-vis spectrophotometer, DLS, FT-IR and TEM. *In vitro/in vivo* studies were also carried out to determine cell viability, uptake, localization and evaluation of anti-tumor efficacy with biosafety.

RESULTS: The fabricated nanocomposites were successfully coated with polymer. A nearly zero premature drug release at physiological pH/temperature was achieved. In addition, *in vitro/in vivo* study exhibits that

synthesized nanocomposites enables to deliver promising synergistic chemo-photothermal treatment.

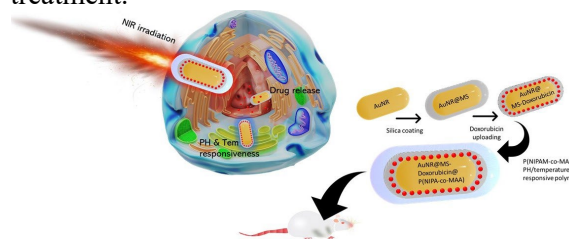


Fig. 1. Schematic diagram of research plan.

DISCUSSION & CONCLUSIONS: The successful coating of synthesized nanocomposites were confirmed by measuring surface charge and using FT-IR. Furthermore, it was sowed a nearly premature drug release at physiological pH/temperature. The synthesized nanocomposite could be successfully and effectively delivering synergistic chemo-photothermal treatment into target site, compared with individual cancer treatment.

REFERENCES: [1] Z. Zhang et al., Adv. Mater., **2012**, v. 24, p. 1418; [2] J. Liu et al., Small, **2015**, v. 11, p. 2323; [3] Vankayala et al., Biomaterials, **2014**, v. 35, p. 5527.

Unravelling the Behaviour of Octacalcium Phosphate in Various Model Solutions

I. Kovrlija¹, J. Locs^{1,2}, D. Loca^{1,2}

¹*Rudolfs Cimdins Riga Biomaterials Innovation and Development Centre, Institute of General Chemical Engineering, Faculty of Materials Science and Applied Chemistry, Riga Technical University, Riga, Latvia,* ²*Baltic Biomaterials Centre of Excellence, Headquarters at Riga Technical University, Riga, Latvia.*

INTRODUCTION: Octacalcium phosphate (OCP) has proven to be one of the extremely important orthophosphates. Characteristics behind OCP are the ones continuously pushing it in the foreground of bone engineering [1]. Its complex structure, possibility to transform to calcium deficient hydroxyapatite (CDHAp), and ability to be further ameliorated are especially beneficial in *in vitro* and *in vivo* studies [2]. Nevertheless, in order to be able to ascribe the beneficial effects to OCP, it is essential to validate its behaviour in key model solutions. The aim of this study was to show the changes in OCP structure in three different media, during the period of 30 days.

METHODS: Octacalcium phosphate powder was obtained through the hydrolysis of α -tricalcium phosphate (α -TCP). 9 g of α -TCP was immersed in 4.5 L of orthophosphoric acid (H_3PO_4). The suspension was stirred continuously for 9 days and the obtained product was washed and dried overnight at 37 °C. OCP powders were immersed in Dulbecco's modified Eagle's medium (DMEM), phosphate-buffered saline (PBS) and osteogenic media in 1:60 weight to volume ratio. Soaking of the powders was conducted in plastic plates at 37 °C, for 30 days, in a thermostat. Model solutions were replaced every seven days. Every set of samples (7, 14, 21 and 30-day time point) was washed with deionized water and dried overnight. Phase composition of the powders was analyzed using X-ray diffractometer, while the morphology of powders was determined by a scanning electron microscope (SEM).

RESULTS: XRD and SEM have shown that the product obtained after the hydrolysis was octacalcium phosphate. Samples soaked in model solutions have preserved the characteristic attributes of OCP, however the slight increase of CDHAp phase indicated the partial hydrolysis of OCP that has transpired.

DISCUSSION & CONCLUSIONS:

Evaluation of the behaviour that OCP has in different model solutions was an important step in the overall scheme of OCP functionalization. Each model solution was carefully chosen due to the heavy usage in *in vitro* cell studies and the pivotal role they have in examining the pro-osteogenic effect of OCP. The study has revealed that OCP attained its main characteristics, with a strong tendency for hydrolysis to apatite phase, highly desirable during the initial stages of new bone formation.

ACKNOWLEDGEMENTS: This project has received funding from the European Union's Horizon 2020 research and innovation programme under the Marie Skłodowska-Curie grant agreement No 860462 (PREMUROSA).

REFERENCES: [1] I. Kovrlija et al., *Acta Biomater.*, **2021**, v. 135, p. 27; [2] Y. Shiwaku et al., *LTD*, **2020**.

Assessment of Skin Permeation of Caffeic Acid from Solid Lipid Nanoparticles and Ethosomes

S.S. Hallan^{1,2}, A. Brangule^{1,2}, T. Ruzgas³, R. Cortesi⁴, E. Esposito⁴

¹Riga Stradins University, Department of Pharmaceutical Chemistry, Riga, Latvia, ²Baltic Biomaterials Centre of Excellence, Headquarters at Riga Technical University, Riga, Latvia,

³Biofilms - Research Center for Biointerfaces, Malmö University, Malmö, Sweden,

⁴Department of Chemical, Pharmaceutical and Agricultural Sciences, University of Ferrara, Ferrara, Italy

INTRODUCTION: The study was aimed at incorporation of caffeic acid (CA) into solid lipid nanoparticles (SLN) and ethosomes (ETHO) to excel its therapeutic potential and delivery across the skin barrier.

METHODS: The effect of lipid matrix has been investigated based on morphology by cryogenic transmission electron microscopy and small angle X-ray scattering, while the dimensions have been measured by photon correlation spectroscopy. The antioxidant potential has been assessed by the 2, 2-diphenyl-1-picrylhydrazyl methodology. The influence of the type of nanoparticulate system on CA diffusion has been estimated by Franz cell associated to nylon membrane, though to evaluate CA permeation through the skin, an amperometric study has been conducted, based on porcine skin covered oxygen electrode (SCOE). The assembly permits to measure the O₂ concentration changes in the skin membrane induced by polyphenols- free radical reactions (Fig. 1). Furthermore, skin resistance was measured to understand interactions of both nano systems with skin membrane using electrochemical impedance spectroscopy (EIS).

RESULTS: Franz cell results revealed that CA diffusion from ETHO was 18-fold slower than SLN. The amperometric approach confirmed the transdermal delivery effect of ETHO, signifying an intense antioxidant activity of CA and a very small response in the case of SLN. Moreover, reversible interactions between nano systems and skin were found and ETHO have shown better blending with skin lipids, hindered the movements of ions and increased the skin resistance. Lastly, SLN and ETHO have passed an irritation patch test on 20 human volunteers.

DISCUSSION & CONCLUSIONS: On encapsulation of phenolic molecule with maintained antioxidant power, ETHO can better protect CA against degradation, as compared to SLN. Indeed, this *ex-vivo* model emphasized

the transdermal potential of ETHO-CA that promoted CA antioxidant activity through the skin.

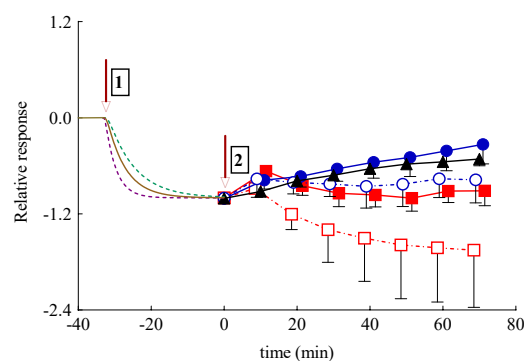


Fig. 1: Relative, average amperometric current response of SCOE immersed in citrate buffer saline (pH 5.5) upon the addition of 0.5 mM of both H₂O₂ (arrow 1) and CA (arrow 2) in solution (black triangles), ETHO (blue closed circle) and SLN (red closed squares). Whereas unloaded ETHO and SLN in blue open circles and red open squares respectively.

Furthermore, the catalase/ peroxidase modified oxygen electrode enabled to demonstrate the delivery of antioxidant effect by SLN-CA, which was not feasible with SCOE. Therefore, a versatile strategy should be developed to assess the effectiveness of drug delivery systems.

ACKNOWLEDGEMENTS: This research was funded by the University of Ferrara (FIR 2019 and FAR 2019).

REFERENCES: [1] Hallan et al., *Pharmaceutics*, **2020**, v. 12, p. 740; [2] Sguizzato et al., *Nanomaterials*, **2020**, v. 10, p. 961.

The Use of Methacrylated Silk-Fibroin/PLGA Spheres for The Delivery of Anti-inflammatory and Osteogenic Dual-drug Symbols is Promise for Bone Regeneration

J. Amirian^{1,2}, A. Brangule^{1,2}, D. Bandere^{1,2}

¹Riga Stradins University, Department of Pharmaceutical Chemistry, Riga, LV, ²Baltic Biomaterials Centre of Excellence, Headquarters at Riga Technical University, Riga, LV

INTRODUCTION: Designing of composite materials with excellent biocompatibility, biodegradability and controlled drug release properties is vital for tissue engineering. In recent years, poly[lactic-co-(glycolic acid)] (PLGA) based synthetic polymers have been widely used in medical applications such as suture materials, implants, and controlled drug delivery systems. Furthermore, natural protein, Silk-Fibroin (SF), produced by *Bombyx mori*, has been used in a variety of biotechnological and medical applications. Simvastatin as an osteogenic drug stimulates osteogenesis by inducing the expression of osteogenic-related gene BMP-2; dexamethasone (DEX) as an anti-inflammatory drug has an important role in the bone regeneration. In this study, our goal was to determine the most effective and optimal drug delivery system for bone regeneration by combining SFMA-DEX hydrogel and PLGA-SIM sphere with different ratios, in order to find the best drug delivery system for bone regeneration.

METHODS: In this study, first simvastatin (SIM), a drug that promotes bone regeneration, was encapsulated in the PLGA spheres to ensure a long-term and sustained release of the drug. In the following steps, silk-fibroin was extracted from *Bombyx mori* and used to prepare and synthesize methacrylated silk-fibroin (SFMA), a hydrogel carrier for PLGA-SIM particles. There are two drugs, dexamethasone and simvastatin, which are used as model drugs. The simvastatin is encapsulated in PLGA spheres, while the dexamethasone is directly dispersed in SFMA hydrogels (SFMA-DEX). Followed by crosslinking under the control of a photo-initiator and UV illumination. We examined each hydrogel system using scanning electron microscopy (SEM) and Fourier transform infrared spectroscopy (FT-IR). Additionally, we evaluated the simvastatin release from each hydrogel system. Other properties, such as swelling behavior and degradation, depend on the composition of each system. CCK-8 tests

were used for the *in vitro* experiments, while fluorescent microscopy was used to test cell proliferation.

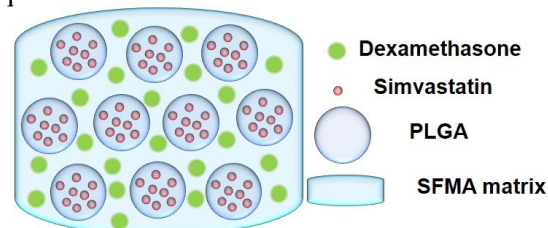


Fig. 1: Anti-inflammatory and osteogenic Dual-drug delivery system loaded in SFMA hydrogel- and PLGA spheres.

DISCUSSION & CONCLUSIONS: The dual drug delivery systems with the anti-inflammatory and osteogenic drugs promote the bone regeneration without foreign body reaction, and therefore, allow a higher rate of bone regeneration. At the end this composition can be used as promising bioink for 3D printing of the tissue and organs.

ACKNOWLEDGEMENTS: This project has received funding from the European Union's Horizon 2020 research and innovation programme under the grant agreement No 857287

REFERENCES: [1] H. Zheng, and B. Zuo, Journal of Materials Chemistry B. **2021**, v. 9, p. 1238; [2] I. Fasolino et al., Materials science and Engineering: C, **2019**, v. 105, 110046.

Development and Stability of Silk fibroin/Calcium Phosphate/Gelatin/Horseradish Peroxidase Hydrogels

A. Grava^{1,2}, A. Dubnika^{1,2}

¹RTU Rudolfs Cimdins Riga Biomaterials Innovation and Development Centre, Faculty of Materials Science and Applied Chemistry, Riga Technical University, Riga, LV, ²Baltic Biomaterials Centre of Excellence, Headquarters at Riga Technical University, Riga, Latvia

INTRODUCTION: Nowadays, more and more composites resembling natural bone are produced. One of them is silk fibroin (SF) and calcium phosphate (CaP) composite [1]. In this composite, SF provides biocompatible organic phase, while CaP mimics the inorganic, mineral phase. Gelatin (G) can be added to *in situ* synthesized SF/G composite to provide higher mechanical properties. However, horseradish peroxidase (HRP) and hydrogen peroxide (H₂O₂) are used as non-toxic crosslinking agent to obtain hydrogels. Altogether a novel, bone regenerative matrix can be developed.

METHODS: Prior to hydrogel preparation, SF/CaP *in situ* synthesis was performed. 10 mg/mL SF solution was added to calcium oxide (CaO), then 2M orthophosphoric acid (H₃PO₄) was added dropwise until pH 6, 8, 10 and 11 was achieved. Afterwards 100 mg/mL G was added to SF/CaP slurry and set aside to bloom. Then SF/CaP/G mixture was heated to 60 °C and dissolved. 1 mL of the mixture was transferred to each well in 24-well plate, where 10 µL of each HRP and H₂O₂ were added with pipetting. The prepared hydrogels were put into the incubator at 37°C to crosslink for 5 days. Lastly, hydrogels were frozen and lyophilized. The obtained SF/CaP composites were characterized with XRD, FT-IR, BET and SEM analysis, while hydrogel gel fraction, swelling and morphology analysis was made.

RESULTS: After XRD phase analysis, it could be concluded that at pH 6 and 8 brushite and hydroxyapatite composite was made, on the other hand at pH 10 and 11 pure hydroxyapatite was synthesized. The specific surface area (SSA) did not differ in between the samples, which means that CaP type did not affect it. Composite synthesized at pH 8 - 66.97±6.27 m²/g had the highest SSA, but the lowest SSA was for the other brushite containing composite obtained at pH 6 - 57.78±5.03 m²/g. Developed hydrogels with hydroxyapatite had higher gel fraction and swelling degree. Swelling degree of hydrogels synthesized at pH 10 was

956.32±18.20% and gel fraction 107.30±25.70%. Contrastingly swelling degree of hydrogel without CaP was 539.53±60.97% and gel fraction 0.9113±0.6261%. The achieved hydrogels had an uneven pore distribution (Fig 1), which is linked to freezing method.

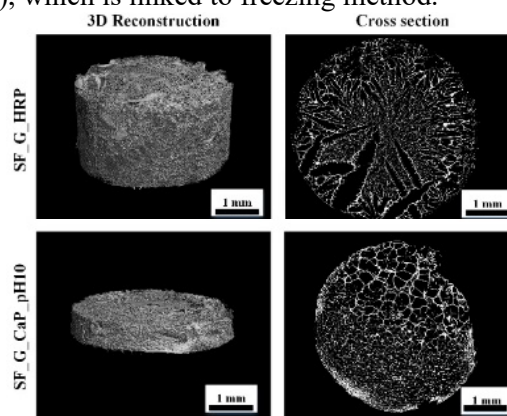


Fig. 1: SF/CaP/G/HRP hydrogel morphology.

DISCUSSION & CONCLUSIONS: From the obtained results it could be concluded that CaP phase has an impact on SF/CaP/G/HRP stability. Hydrogels with hydroxyapatite (pH 10 and 11) showed higher gel fraction than hydrogels with brushite (pH 6 and 8), thus indicating the importance of CaP phase in crosslinked matrix. Samples without CaP showed 60% lower gel fraction. Swelling properties of the obtained hydrogels appeared the same as gel fraction – hydrogels with hydroxyapatite had higher swelling degree.

ACKNOWLEDGEMENTS: This research has received funding from the European Union's Horizon 2020 research and innovation programme under the grant agreement No 857287 and the M-era.Net 2 project "Bioactive injectable hydrogels for soft tissue regeneration after reconstructive maxillofacial surgeries" (INJECT-BIO) under agreement No. ES RTD/2020/14

REFERENCES: [1] J. Mobika et al., J. Mol. Struct., 2020, v. 1206, 127739.

Covalently Bonded ϵ -Polylysine/Hyaluronic Acid Hydrogels with Enhanced Antibacterial Action

A. Sceglavs^{1,2}, C. Siverino³, F.T. Moriarty³, K. Salma-Ancane^{1,2}

¹Rudolfs Cimdins Riga Biomaterials Innovations and Development Centre of RTU, Riga, Latvia, ²Baltic Biomaterials Centre of Excellence, Headquarters at Riga Technical University, Riga, Latvia, ³AO Research Institute Davos, Davos, Switzerland

INTRODUCTION: Post-operative wound care is usually accompanied by bacterial infection. The excessive use of synthetic antibiotics can lead to multidrug-resistant bacterial infections in clinic. Natural polymer-based antibacterial hydrogels could be a new alternative to conventional antibiotic treatments. One of such bio-polymers is ϵ -polylysine (ϵ -PL) that possesses high antibacterial activity against both Gram-negative and Gram-positive bacteria. However, structural modification of ϵ -PL is required to synthesize hydrogels. Such modification approaches can significantly lower antibacterial properties of ϵ -PL. The aim of this work is to study the antibacterial properties of chemically crosslinked hydrogels composed of antibacterial ϵ -PL and bio-intrinsic hyaluronic acid (HA).

METHODS: Copolymeric hydrogels comprised of ϵ -PL and HA were synthesized by 1-ethyl-3-(3-dimethylaminopropyl) carbodiimide N-hydroxysuccinimide (EDC/NHS) based covalent crosslinking. The ϵ -PL/HA hydrogels were synthesized with ϵ -PL to HA mass ratio of 40:60 wt%, 50:50 wt%, 60:40 wt%, 70:30 wt%, 80:20 wt% and used for further investigations. To perform antibacterial properties for ϵ -PL pure compound and PL/HA hydrogels, microorganisms as *E. coli* (ATCC 25922) and *P. aeruginosa* 9 as Gram-negative bacteria and *S. aureus* JAR (010631), *S. epidermidis* (ATCC 35984) and *S. pyogenes* (ATCC 19615) as Gram-positive bacteria were chosen. The obtained data from various studies were processed using IBM SPSS statistical software.

RESULTS: Preliminary experiments revealed ϵ -PL antibacterial activity reducing bacteria concentration for 99,999% in terms of minimal inhibitory and bactericidal concentrations (MIC/MBC). However, ϵ -PL showed different MIC/MBC values for the different strains used. The antibacterial tests revealed that ϵ -PL/HA hydrogels with increasing ϵ -PL mass ratio starting from 50 wt% showed statistically significant bacterial reduction against pure

bacteria as negative control ($p < 0.05$). Both fast (up to 24 h) and prolonged (up to 7 days) antibacterial activity were evaluated for the synthesized ϵ -PL/HA hydrogels.



Fig. 1: ϵ -PL/HA hydrogels – wet (left) and dry (right) samples

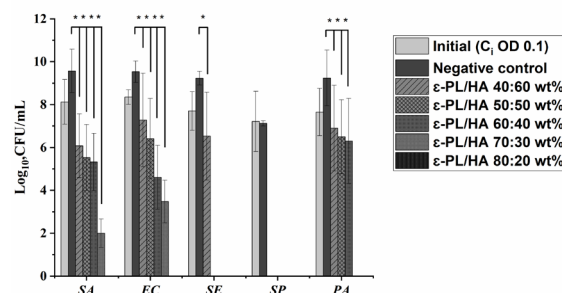


Fig. 2: Results of broth microdilution method for ϵ -PL/HA hydrogels in dynamic conditions (SA-*S. aureus*; EC-*E. coli*; SE-*S. epidermidis*; SP-*S. pyogenes*; PA-*P. aeruginosa*), $n=3$; $p < 0.05$.

DISCUSSION & CONCLUSIONS: Covalently crosslinked ϵ -PL/HA hydrogels were synthesized via amide linkage. The ϵ -PL/HA hydrogels demonstrated promising broad spectrum antibacterial activity against Gram-positive and Gram-negative bacteria. However, viscoelastic properties and cell viability assays should be performed to evaluate the potential application of the fabricated hydrogels in tissue engineering field.

ACKNOWLEDGEMENTS: This project has received funding from the European Union's Horizon 2020 research and innovation programme under the grant agreement No 857287. The authors acknowledge financial support from the Latvian Council of Science research project No. lzp2020/1-0072 "Injectable bioactive biocomposites for osteoporotic bone tissue regeneration (inBioBone)".

Development of Antibacterial Hyaluronic acid-based Hydrogels

K. Aunina^{1,2}, D. Loca^{1,2}, A. Ramata-Stunda³, V. Nikolajeva³

¹Rudolfs Cimdins Riga Biomaterials Innovations and Development Centre of RTU, Institute of General Chemical Engineering, Faculty of Materials Science and Applied Chemistry, Riga Technical University, Riga, LV, ²Baltic Biomaterials Centre of Excellence, Headquarters at Riga Technical University, Riga, LV, ³Department of Microbiology and Biotechnology, Faculty of Biology, University of Latvia, Riga, LV

INTRODUCTION: Nowadays, there is a growing interest among scientists in developing biomaterials that provide local antibacterial effect. Due to this necessity, reducing the potential risk of infection, as well as decreasing the need for antibiotics is of pivotal value. ϵ -Polylysine (ϵ -PL), a water soluble and non-toxic compound, could provide local antibacterial effect [1]. Furthermore, hyaluronic acid (HA), which is being widely used in biomedicine field because of its biocompatibility and high-water binding capacity [2], could serve as a base material for hydrogel preparation. By combining these two polymers it could be possible to form physically cross-linked hydrogels for tissue engineering. Hence, the main objective of the current research was to prepare antibacterial HA-based hydrogels and characterize them towards gel fraction, cell viability, and antibacterial properties.

METHODS: HA/ ϵ -PL hydrogels, with different HA content (HA: ϵ -PL 40:60; 50:50 and 60:40), were synthesized via polyelectrolyte complexation. Insoluble part of prepared samples was determined in 200 mL of deionized water at 37 °C for 48 h. The antibacterial efficacy of prepared HA/ ϵ -PL hydrogels was evaluated using the zone of inhibition tests against *Escherichia coli* (*E. coli*). 3T3 cell line was used for *in vitro* biocompatibility assessment in the direct contact with HA/ ϵ -PL hydrogels.

RESULTS: Increasing the HA content in the prepared HA/ ϵ -PL compositions, the insoluble part values increased from 52±2% up to 78±2% (HA/ ϵ -PL 40:60-60:40). In the cell viability assay, all three compositions showed negative cell response, reducing viability by more than 40 %. Lower ϵ -PL content results in better viability. The sterile zone diameter increased from 17±1% up to 21±1% (HA/ ϵ -PL 40:60-60:40) with an increase of ϵ -PL content in samples (Fig. 1).

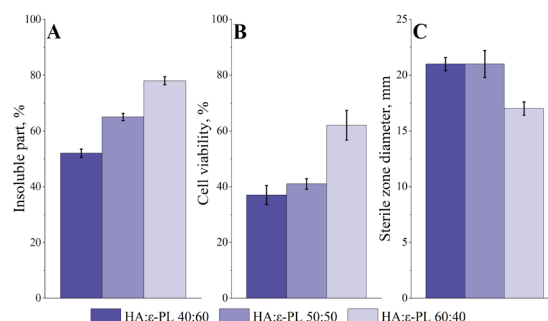


Fig. 1: Effect of HA content in HA/ ϵ -PL hydrogels properties: A Insoluble part; B Cell viability; C Sterile zone diameter.

DISCUSSION & CONCLUSIONS: During the research it was established that HA/ ϵ -PL hydrogels have the ability to inhibit growth of *E. coli*, which is a gram-negative bacterium. However, further research is necessary to find the optimal HA/ ϵ -PL ratio to ensure both antibacterial properties and a positive cellular response.

ACKNOWLEDGEMENTS: The authors acknowledge financial support from the Latvian Council of Science research project No. Izp-2019/1-0005 “Injectable in situ self-crosslinking composite hydrogels for bone tissue regeneration (iBone)” and from the European Union’s Horizon 2020 research and innovation programme under the grant agreement No 857287 (BBCE).

REFERENCES: [1] S.C. Shukla et al., *Biochem. Eng. J.*, **2012**; v. 65, p. 70; [2] A. Fallacara et al., *Polymers (Basel)*, **2018**, v. 10(7), p. 701.

Calcium Phosphate Cement Additives. Scientific vs. Patent Literature

A. Vezenkova¹, J. Locs^{1,2}

¹Rudolfs Cimdins Riga Biomaterials Innovations and Development Centre of RTU, Institute of General Chemical Engineering, Faculty of Materials Science and Applied Chemistry, Riga Technical University, Riga, LV, ²Baltic Biomaterials Centre of Excellence, Riga, LV

INTRODUCTION: Finding the right properties for calcium phosphate cement (CPC) to be osteoinductive, as well as injectable and suitable for clinical use is still a crossroad puzzle, even despite the years-long research and several products having already reached the market. To improve the chances of developing a surgically applicable material different additives are being used. Scientific publications are not the only source where to look for new developments in a particular field of interest. Information on different additives used in CPCs, as presented in patent literature, is also of value.

METHODS: Recent patents with grant date or patent applications with earliest priority date starting from 2017 were chosen, searching in *Espacenet* by keywords ‘injectable calcium phosphate’, ‘injectable osteoinductive porous calcium phosphate’ and ‘porous calcium phosphate’. Search results were evaluated, and most relevant documents were reviewed and compared with information in scientific publications.

RESULTS: Patents or patent applications, protecting or aiming to protect calcium phosphate cements modified with PEG cladding photosensitizer IR780, gelatin, chitosan, hydroxypropylmethylcellulose, carboxymethylcellulose, zirconium phosphate, chondroitin sulphate, lanthanides, strontium, growth factors, pore generating proteins, polyanhydride, calcium sulphate, sodium phosphate, ammonium salt, and bioactive glass, hydrogel, citric acid and fibres were found and compared with information about these additives provided in scientific literature.

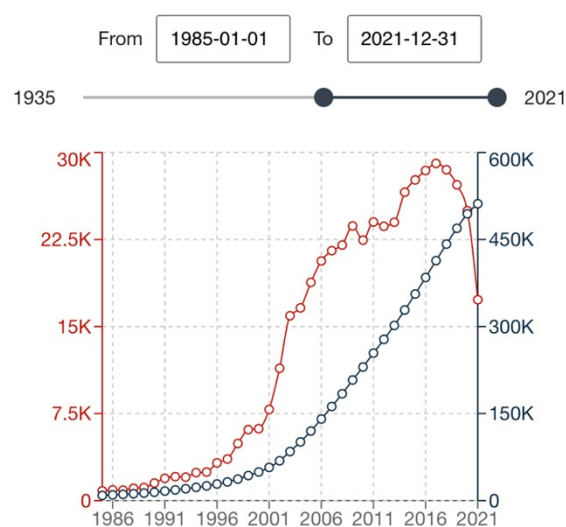


Fig. 1: Espacenet data on the amount of patent documents found using “injectable calcium phosphates” as a search term (red line – count; blue line – cumulative count).

DISCUSSION & CONCLUSIONS: The large amount of patent applications shows that the field is still in development and there is place left for new research to be conducted. Recently patents have been granted to complex compositions, with more than two ingredients. Patent and patent application documents should be read with caution, since information is often presented in a manner that allows patent proprietors to obtain the broadest possible protection for their inventions. Although, both scientific publications and patent literature provide information about the same additives, scientific publications usually discuss the impact of each additive in more specific detail.

ACKNOWLEDGEMENTS: The authors acknowledge financial support from the European Union’s Horizon 2020 research and innovation programme under the grant agreement No 952347 (RISEus2).

Nanostructured Polyacrylamide Hydrogels with Antimicrobial Performances and Mineralization Potential

E. Olaret¹, R. Oprea¹, S.I. Voicu¹, A. Serafim¹

¹Faculty of Chemical Engineering and Biotechnologies, University Politehnica of Bucharest, Bucharest, RO

INTRODUCTION: This study presents the facile fabrication of nanostructured viscoelastic polyacrylamide (PAAm) hydrogels with mineralization potential and antimicrobial activity. Following silver (Ag) decoration, the carbon nanotubes (CNT) were embedded in the semi-interpenetrated network of linear PAAm entrapped in the cross-linked 3D network of the same polymer (Fig. 1).

METHODS: Several nanostructured hydrogels were synthesized using different ratios of Ag decorated CNT (Ag@CNT) (S series, see Table 1). Their antimicrobial activity was assessed against both Gram-negative (*E. Coli*) and Gram-positive (*S. aureus*) species using the indirect contact method. For comparison, composites with non-decorated CNTs were also synthesized (M series).

The ability of the materials to mineralize upon incubation in simulated body fluid (SBF) was also investigated and the influence of the mineral formation on the mechanical properties was evaluated through uniaxial compression tests.

The micro-architectural features of the nanostructured scaffolds, before and after 4 weeks of incubation in SBF, were investigated using micro-computed tomography (μ CT).

RESULTS: PAAm-Ag@CNT composites were synthesized following a simple procedure, as schematically described in Fig. 1.

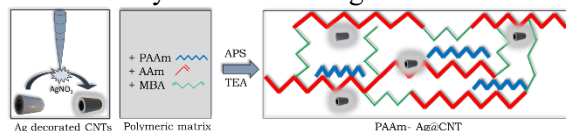


Fig. 1: Schematic depiction of the PAAm-Ag@CNT hydrogels synthesis.

The antimicrobial tests showed that only the hydrogels with an AAm:Ag@CNT filling ratio above 100:0.5 have antimicrobial activity against both types of tested bacteria (table 1).

Table 1. Synthesis details and antimicrobial activity (%) of the nanostructured materials.

	AAm: Ag@CNT	AAm: CNT	<i>E. Coli</i>	<i>S. Aureus</i>
C	100:0	100:0	5	5
S1	100:0.125	-	25	25
S2	100:0.25	-	35	50
S3	100:0.5	-	95	98
S4	100:1	-	99	100
M1	-	100:0.125	5	5
M2	-	100:0.25	15	5
M3	-	100:0.5	10	5
M4	-	100:1	10	10

Following 4 weeks' incubation in SBF, a stiffening of the samples was noticed, which may be assigned to mineral formation (Fig. 2).

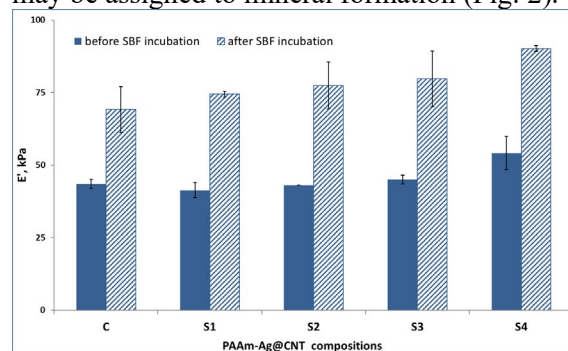


Fig. 2: Compression modulus before and after incubation in SBF (4 weeks).

DISCUSSION & CONCLUSIONS: Our results indicated that loading less than 100:0.5 AAm:Ag@CNT does not modify the physical and architectural characteristics of the control sample. Increasing the loading ratio to AAm:Ag@CNT 100:1 leads to more robust hydrogels, with pronounced anti-microbial character against both Gram-positive and Gram-negative species.

ACKNOWLEDGEMENTS: The research was supported through project NanoSHAC within PNCDI III, PN-III-P1-1.1-TE-2019-1161.

Antibacterial Hydrogels as a Particle Formulation

E. Blomstrand^{1,2}, A.K. Rajasekharan², S. Atefyekta², M. Andersson¹

¹Department of Chemistry and Chemical Engineering, Chalmers University of Technology, Gothenburg, SE, ²Amferia AB, AZ BioVentureHub, Mölndal, SE

INTRODUCTION: Antimicrobial peptides (AMPs) are a vital part of our innate immune system and should be able to defend the host from a broad spectrum of pathogens [1]. Despite the well documented effect of AMPs, they remain poorly translated to medical applications. The most challenging reason for this is their low stability towards proteolytic degradation [2]. Here we present a concept of covalently attaching AMPs to microscopic particles made from a soft polymeric hydrogel. This shields the AMPs from degrading enzymes, while at the same time creating a high surface area with antimicrobial properties. Such a material would be ideal for combating bacterial infections without relying on conventional antibiotics.

METHODS: An acrylated version of the block copolymer Poloxamer 407 was mixed with water and photo initiator to form a gel which was polymerized by exposure to UV light. The hydrogel was then mechanically reduced in size to microscopic particles. The particles were then modified by covalently attaching AMPs to the surfaces utilizing EDC & NHS coupling. The antibacterial effect was evaluated by spreading AMP-modified and non-modified (control) particles on top of an agar plate streaked with *Staphylococcus aureus*. After an overnight incubation, the bioburden beneath each spread was evaluated. Biopsy punches were taken from the middle of each section (both agar and particles were collected) and the CFU/cm² was measured.

RESULTS: The bacterial lawn with the different particles on top after incubation is shown in Fig. 1a. The measured bioburden from biopsy punches taken in the middle of each section is presented in Fig. 1b. The control section showed a bacterial concentration of 2.0×10^9 CFU/cm² and the AMP-modified section showed a bacterial concentration of 1.3×10^5 CFU/cm². In other words, a log 4 reduction was observed for the AMP-modified particles compared to the control particles.

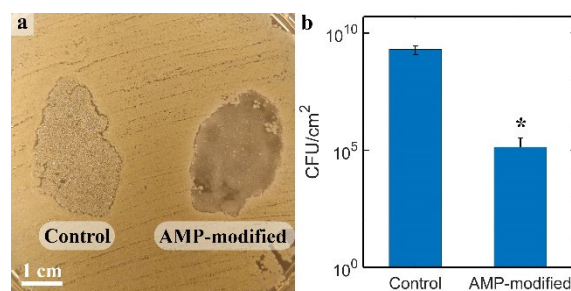


Fig. 1: a) An image of how the agar plates looked like after incubation with the control particles (left) and the AMP-modified particles (right). b) The CFU/cm² corresponding to biopsy punches taken from the middle of the spreads seen in a). * Indicates statistically significant difference to the control with a 95% confidence interval, n=9.

DISCUSSION & CONCLUSIONS: By utilizing a formulation of hydrogel particles with covalently attached AMPs, an antibacterial material was obtained, which can be used to combat bacterial infections in places that are difficult to reach, such as a deeper wound. The strong antibacterial effect observed with this method indicated that AMPs can be a promising alternative to conventional antibiotics and therefore provide a step in the right direction in the fight against antibiotic resistance.

REFERENCES: [1] M. Zasloff, *Nature*, **2002**, v. 415(6870), p. 389; [2] A.T. Yeung et al., *Cellular and Molecular Life Sciences*, **2011**, v. 68(13), p. 2161.

Residual Stresses in an Additively Manufactured Biodegradable Magnesium Alloy

L. Larsson¹, H.N. Åhman^{1,2}, T. Maimaitiyili², C. Persson¹

¹Department of Materials Science and Engineering, Uppsala University, Uppsala, SE,

²Swerim AB, Stockholm, SE

INTRODUCTION: A major limitation of novel biodegradable magnesium (Mg) alloys, destined for degradable implants, is their high corrosion rate. One factor that is known to negatively affect the degradation of metallic parts is the presence of residual stresses built up in the material during processing. Additive manufacturing (*i.e.*, 3D-printing) technique such as Powder Bed Fusion – Laser Beam (PBF-LB) is known to induce the formation of complex residual stress, because of the unique thermal history resulting from the technique. Accurately characterising the residual stress forming in Mg-alloys produced by PBF-LB is therefore crucial for understanding and controlling the degradation behaviour of future biodegradable Mg-based implants.

METHODS: In this study, the residual stress of samples printed in an EOS M100 machine with gas-atomized spherical powder of biodegradable rare-earth magnesium alloy WE43 (Mg-4wt%Y-3wt%Nd-0.5wt%Zr, NMD GmbH) was studied. Because of texture effects (PBF-LB process) and anisotropic properties (hexagonal close packed crystal structure of Mg) of the as-built samples, high energy synchrotron diffraction with high spatial resolution and penetration depth was used to characterize the local residual stress. Neutron imaging was used to map the strain in the complete sample and neutron diffraction was performed to validate the imaging results. The influence of PBF-LB process parameters (Fig. 1) on the residual stress was evaluated.

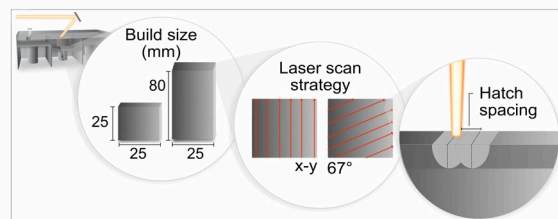


Fig. 1: Schematic illustration of the process parameters under study.

RESULTS: The residual stress formed during PBF-LB was found to be tensile closer to the edges of the as-built samples (P2 vs. P4 in

Fig. 2). In the build direction, the larger samples presented a higher degree of residual stress. The difference in build direction was generally found to be larger for samples printed using a 67° scan strategy.

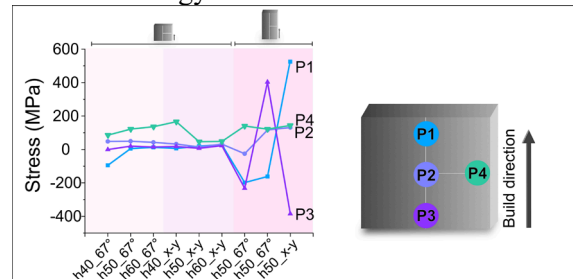


Fig. 2: Influence of process parameters on the residual stress (longitudinal) of the samples. h =hatch distance (μm).

DISCUSSION & CONCLUSIONS: Residual stress in Mg samples produced by PBF-LB was successfully measured by synchrotron and neutron techniques. The presence of tensile stresses is known to accelerate the degradation of the WE43 Mg alloy [1]; here, the stress originating from the PBF-LB process was found to be tensile towards the edge of the sample and can thus have an impact on the degradation behaviour. This, together with the high degree of residual stress detected in larger builds (which can lead to cracking during/after the PBF-LB process), highlights the need for post-processing in terms of stress relief treatments, *e.g.* thermal treatments.

ACKNOWLEDGEMENTS: The authors gratefully acknowledge funding from the Swedish Foundation for Strategic Research (SSF) within the Swedish national graduate school in neutron scattering (SwedNess), and VINNOVA's Competence Centre in Additive Manufacturing for the Life Sciences AM4Life (2019-00029).

REFERENCES: [1] M. Esmaily et al., *Addit. Manuf.*, **2020**, v. 35, p. 1.

Freeze-dried Composition of Alginate and Bioglass as an Engineered Environment for the Osteosarcoma Model

K. Menshikh¹, I. Kovrlija², M. Miola³, A. Cochis¹, L. Rimondini¹

¹Center for Translational Research on Autoimmune and Allergic Disease, Università del Piemonte Orientale, Novara, IT, ²Institute of General Chemical Engineering, Rudolfs Cimdins Riga Biomaterials Innovation and Development Centre, Riga, LV, ³Institute of Materials Engineering and Physics, Politecnico di Torino, Turin, IT

INTRODUCTION: Rapidly developing field of tumour engineering nowadays provides a variety of solutions to simulate different types of cancer *in vitro*. However, there is a lack of robust *in vitro* models for hard tissue cancers such as osteosarcoma. This work aims to find an approach for providing osteosarcoma cell spheroids with the necessary biomechanical environment needed for adequate cell behaviour and, thus, reliable response to anticancer drugs.

METHODS: To obtain stable spheroids, human osteosarcoma cells (U2OS) were cultured in a multiwell plate, coated with 1% agarose gel, in standard conditions of 37°C and 5% carbon dioxide (CO₂) content. The dynamics of cell metabolic activity in spheroids was monitored by resazurin reduction assay, and the morphology of spheroids was assessed visually by light microscopy, as well as by fluorescent microscopy using the live/dead and DAPI staining. Alginate and bioglass were the components of choice for producing the bone-like scaffold due to their good recognition in the field of biomaterials. Bioglass particles differing in size (100 and 500 nm in diameter) were tested along with alginate in different ratios, volumes and gelation periods. After the onset of polymerization via soaking in calcium chloride (CaCl₂), samples were frozen either at -20°C or -80°C overnight and freeze-dried during various periods. The optimal parameters were chosen based on the analysis with scanning electron microscopy (SEM), supplemented with element mapping. Prior to arranging the cell spheroids inside the obtained porous matrices, the latter were sterilized in ethanol and pre-soaked in culture media.

RESULTS: Throughout the set-up of the method, and considering the data from the aforementioned analyses, the final optimal parameters and the content of alginate and bioglass were established. The chosen matrices possessed sufficient mechanical characteristics, and architecture was comparable to that of the

trabecular bone tissue in terms of porosity and spatial arrangement (Fig. 1). The bioglass particles were shown to be evenly distributed with the maintenance of the initial morphology. The viability of spheroids, estimated by resazurin reduction assay, as well as morphological analysis conducted with the help of histological methods, allowed us to conclude that the obtained scaffolds are suitable as an environment for 3D *in vitro* culture.

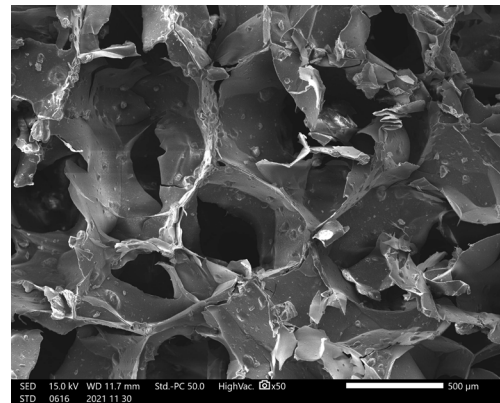


Fig. 1: Morphology of freeze-dried scaffold composed of 4% alginate solution and bioglass particles ($d = 100$ nm), cross-section, SEM.

DISCUSSION & CONCLUSIONS: The described approach for creating a proper engineered environment for the osteosarcoma model can be admitted as promising in terms of developing antitumor drug test systems and studying peculiarities of a pathology of interest. Moreover, the proposed system is tuneable, which offers the possibility of introducing various cell lines and setting up dynamic conditions for further experiments.

ACKNOWLEDGEMENTS: This research was funded by European Union's Horizon 2020 Research and Innovation Program under the Marie Skłodowska-Curie grant agreement No. 860462 - Project PREMURSA.

Calcium Phosphate and Silk Fibroin Biocomposite for Dental Application

V. Zalite¹, J. Locs^{1,2}

¹*Rudolfs Cimdin's Riga Biomaterials Innovation and Development Centre, Institute of General Chemical Engineering, Faculty of Materials Science and Applied Chemistry, Riga Technical University, Riga, Latvia,* ²*Baltic Biomaterials Centre of Excellence, Headquarters at Riga Technical University, Riga, Latvia*

INTRODUCTION: Recently, new method-cold sintering (CSP) is introduced for ceramic material production. The main advantage of CSP is relatively low processing temperatures, allowing to produce nanostructured ceramic materials and even biocomposites from ceramic powders and organic substances [1,2]. Natural tooth enamel is unique biocomposite that consists of inorganic substance hydroxyapatite (HAp), water and organic part proteins. Thereby, CSP could be appropriate technique for production of dental restoration materials, with chemical structure and properties similar to natural enamel. In this study, amorphous calcium phosphate (ACP) and silk fibroin (SF) were chosen for composite production.

METHODS: ACP powder was synthesized *via* reprecipitation method, from CaO, H₃PO₄, HCl and NaOH. SF was obtained as described before [3]. Biocomposites were obtained by mixing 98 wt% of ACP paste with 2wt% of silk fibroin solution (ACP+SF). Mixing was done by Hauschild Speed Mixer 2000 rpm for 2 min. ACP and ACP+SF were subjected to freeze drying process to obtain powders. Afterwards, uniaxial pressing (Ø 13 mm, 1500 MPa, 10 min, room temperature) was used to obtain densified and sintered samples (ACP_1500 and ACP+SF_1500). Characterization of synthesized and treated samples was performed using N₂ adsorption (BET), XRD, helium pycnometry.

RESULTS: XRD pattern of synthesized ACP powder indicated only 2 humps characteristic of ACP phase (one around 25°-35° 2θ and second around 42.5°-55° 2θ). Identical diffractograms were obtained for sintered ACP_1500 and ACP+SF_1500 samples. Specific surface area (SSA) of synthesized ACP powder was 130 g/m² and 153 g/m² for ACP+SF composite powder. Density of powdered samples was 2.44 g/cm³ for ACP and 2.39 g/cm³ for ACP+SF, but after pressing relative density of the samples was 90% for ACP_1500 and 92% for ACP+SF_1500.

DISCUSSION & CONCLUSIONS: XRD data showed that no phase transition occurred during cold sintering process, thus it was possible to obtain densified ACP phase, which is not possible using conventional techniques. Also, it was concluded, that presence of SF has no effect on ACP phase transformation while 1500 MPa pressure was applied, but BET results indicated larger SSA for the sample with SF. To explain this observation, additional measurements need to be done to determine pore size distribution in powdered materials. It could be said that the difference in SSA values of ACP and ACP+SF did not significantly affect the relative density of the ACP_1500 and ACP+SF_1500. In order to gain a full understanding of the properties of obtained materials, it is necessary to perform additional analysis, such as SEM, FTIR and testing of mechanical properties.

ACKNOWLEDGEMENTS: This work has been supported by the European Regional Development Fund, within the Activity 1.1.1.2 "Post-doctoral Research Aid" of the Specific Aid Objective 1.1.1 "To increase the research and innovative capacity of scientific institutions of Latvia and the ability to attract external financing, investing in human resources and infrastructure" of the Operational Programme "Growth and Employment" (No.1.1.1.2/VIAA/3/19/459).

REFERENCES: [1] N. Guo et al., *Materialia*, **2022**; [2] S. Grasso et al., *Advances in Applied Ceramics*, **2020**; [3] A. Grava et al., *Materials*, **2021**.

Photothermal Biofilm Eradication Achieved by NIR-active Plasmonic Nanoaggregate Films

P. Merkl¹, S. Zhou¹, A. Zaganiaris¹, M. Shahata¹, A. Eleftheraki¹, T. Thersleff², G.A. Sotiriou¹

¹Department of Microbiology, Tumor and Cell Biology, Karolinska Institutet, Stockholm, SE

²Department of Materials and Environmental Chemistry, Stockholm University, SE

INTRODUCTION: Plasmonic nanoparticles with strong near infrared (NIR) light absorption have good biomedical potential, due to the ability of this wavelength range to penetrate tissue and so be used for minimally invasive diagnostic and therapeutic devices *in-vivo*. A therapeutic strategy exploited with NIR plasmonic materials is the photothermal effect - absorbed light is converted into heat. The resultant temperature increase can neutralise infections or cancerous tissue. A problematic form of infection, responsible for most medical device related infections, is the microbial biofilm characterised by the protective extracellular polymeric matrix, which it produces. Due to the dense and inhomogeneous nature of biofilms their treatment by typical therapeutic strategies, such as antibiotics, is challenging [1]. This study presents the single-step flame synthesis of plasmonic nanoaggregates of spherical Ag nanoparticles, with tuneable extinction from the visible to NIR wavelengths. The resultant NIR photothermal behaviour is applied as a film for the eradication of established biofilms of *E. coli* and *S. aureus*.

METHODS: Aerosol self-assembly of particle films by flame spray pyrolysis was performed on polydimethylsiloxane coated substrates and encased with a top polymer layer, forming plasmonic photothermal nanocomposite films. The extinction spectra were optimised by varying the silica content of the nanoaggregates. Biofilms of *S. aureus* and *E. coli* were formed on the nanocomposite film surface, irradiated with 808 nm laser light and CFU quantified.

RESULTS: The extinction spectra of the nanoaggregates were optimised to give high NIR extinction and photothermal performance. Under NIR irradiation the films were able to eradicate established biofilms of clinically relevant *E. coli* and *S. aureus* (Fig. 1).

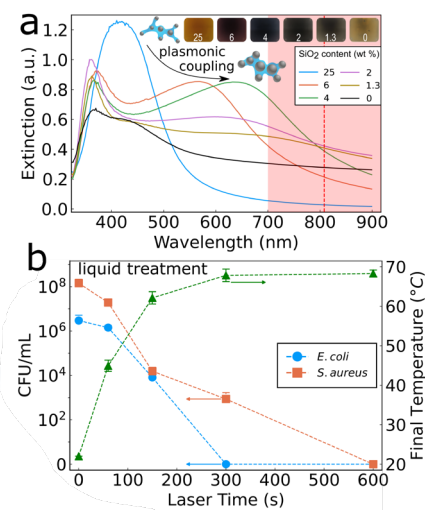


Fig. 1: (a) UV-Vis spectra of plasmonic nanoaggregates with decreasing dielectric spacer SiO₂ content. Inset shows photos taken of the glass slides. (b) Bacteria quantification (CFU/mL) of *E. coli* and *S. aureus* biofilms after NIR laser irradiation and the corresponding temperatures (green triangles, right axis) [2].

DISCUSSION & CONCLUSIONS: The results obtained here demonstrate the facile synthesis of plasmonic silver nanoparticle films with high NIR extinction and photothermal behaviour which under 808 nm laser irradiation completely eradicate bacterial biofilms.

ACKNOWLEDGEMENTS: This project has received funding from the European Research Council (ERC) under the European Union's Horizon 2020 research and innovation program (ERC Grant agreement n° 758705). Funding from the Karolinska Institutet Faculty Board, the Swedish Research Council (2016-03471), the Torsten Söderberg Foundation (M87/18), and the Swedish Foundation for Strategic Research (FFL18-0043) is kindly acknowledged.

REFERENCES: [1] M. Zhou et al., ACS Appl. Mater. Interfaces, **2017**, v. 10, p. 193; [2] P. Merkl et al., ACS App. Nano Mater., **2021**, v. 4(5), p. 5330.

Gold Nanorod-assisted Photothermal Elimination of Bacteria

M. Uusitalo¹, M. Hulander¹, M. Andersson¹

¹Department of Chemistry and Chemical Engineering, Chalmers University of Technology, Gothenburg, SE

INTRODUCTION: Biomaterials-associated infections (BAIs) pose a serious threat in modern healthcare and constitute considerable limitations to the use of biomaterials. Infections associated with biomaterials are generally difficult to manage as they require extended antibiotic treatment and sometimes repeated surgical procedures. One major reason is the formation of a biofilm on the biomaterial surface and the high tolerance to conventional antimicrobial treatments as seen. Along with the emerging problem of antimicrobial resistance, the complications related to BAIs make the development of new ways of preventing or treating these infections of high importance. A possible alternative to conventional antimicrobial treatments for prevention or treatment of BAIs is to photothermally eliminate bacteria using gold nanorods in combination with near-infrared (NIR) light¹. By immobilising gold nanorods on a surface and irradiating with light corresponding to the nanorods' plasmon resonance frequency, the heat released from the nanorods as the plasmons decay can be used to eradicate bacteria growing on the surface.

METHODS: Gold nanorods (66 nm length, 21 nm width) with a maximum longitudinal absorption (between 800-850) nm were synthesised via a wet-chemical, seed-mediated synthesis using hexadecyltrimethylammonium bromide. The gold nanorods were immobilised on glass substrates via electrostatic interactions, and the surface assembly was characterised with scanning electron microscopy (SEM). The antimicrobial activity of the gold nanorod-functionalised glass upon exposure to NIR light was evaluated by culturing *Staphylococcus Aureus* on the surfaces and subsequently irradiating the samples with a NIR laser for 5 min (808 nm, 4 W). Non-irradiated gold nanorod-functionalised glass was used as control. All the samples were stained with LIVE/DEAD BacLight (ThermoFisher) and analysed using fluorescence microscopy.

RESULTS: Surface assembly characterisation with SEM showed an even distribution of gold nanorods with a surface coverage of 16-19 %,

corresponding to 127-149 nanorods/ μm^2 . In Fig. 1 the average percentage of dead bacteria on the surfaces, along with the standard deviation, as determined by image analysis of fluorescence microscopy images, is shown. An antimicrobial activity against *S. Aureus* could be observed for the gold nanorod-functionalised glass irradiated with NIR light, which on average exhibited 45 % dead bacterial cells, compared to the 14 % dead bacteria of the non-irradiated control.

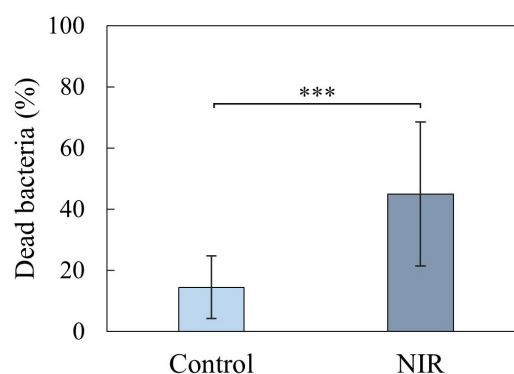


Fig. 1: Antimicrobial activity against *S. Aureus*, determined as percentage of dead bacteria on gold nanorod-functionalised glass irradiated with NIR light. Control is non-irradiated surfaces. *** indicates $P \leq 0.001$.

DISCUSSION & CONCLUSIONS: The initial study shows successful preparation of gold nanorod-functionalised glass surfaces that upon exposure to NIR light exhibit antimicrobial activity against *S. Aureus*, demonstrating the potential of using a combination of gold nanorods and NIR light to photothermally prevent and/or treat biomaterials associated infections.

REFERENCES: [1] M. Pihl et al., Materials Science and Engineering: C, 2017, v. 80, p. 54.

3D-printed Bioengineered Platform for Co-culturing Caco-2/Immune Cells

A.A. Dogan¹, E. Barreto-Durán², K. Pyrc², M. Dufva¹

¹Department of Health Technology, Technical University of Denmark, Kgs. Lyngby, Denmark,

²Małopolska Center of Biotechnology, Jagiellonian University, Kraków, Poland

INTRODUCTION: Epithelial cells, together with immune system cells are crucial cells in maintaining intestinal barrier tissue [1]. These cells are in close contact and influenced by each other. Therefore, investigating the intercellular communication of these cells is very important for understanding intestinal physiology. Previously, three-dimensional (3D)-printed inserts were presented to mimic the intestinal tissue for drug absorption/ transportation studies [2]. In this study, we have designed and fabricated a hydrogel substrate assembled 3D-printed co-culture platform to investigate crosstalk between epithelial and immune cells. Furthermore, we have evaluated the effects of 2D and 3D microenvironments on monocyte differentiation on the platform.

METHODS: The design for the 3D co-culture platform was drawn in Fusion 360 software (Autodesk, USA) and printed in Biomed Clear resin using the Form 3B printer (Formlabs, USA). The printed platform was cleaned with isopropanol followed by UV crosslinking for 2 h at 60 °C and sterilized by autoclaving. Then, gelatin hydrogel substrates were assembled on the 3D-printed platform.

Caco-2 cells were seeded on the gelatin substrate as a monolayer and cultured over three weeks to create barrier function. THP-1 cells were cultured with 50 ng/mL PMA included RPMI 1640 growth medium (10% v/v FBS, 1% v/v Penicillin / Streptomycin) in the 3D gel-like network in the platform. After co-culturing both cell lines, in close contact to each other, immunostaining was performed to characterize the monocyte, differentiated to macrophage in the gel-like network and crosstalk between the cells. Stained cells and co-cultured tissue were imaged using fluorescence microscopy (AxioVision, Zeiss, DE).

RESULTS: The design of the 3D-printed co-culture platform relies on commercially available cell culture plates. The biocompatibility of the 3D-printed platform was studied by co-culturing epithelial cells and macrophages. Caco-2 cells were confluent in week 1 and kept their cobblestone morphologies on the gelatin substrates during

the 3-week incubation. During the 3-day PMA induction period, THP-1 monocytes were differentiated to macrophages (Fig. 1) in the 3D thin hydrogel microenvironment.

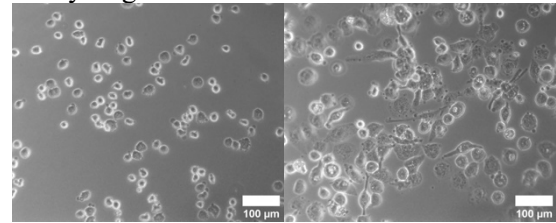


Fig. 1: Differentiation of monocytes in 3D gel-like microenvironment: monocytes (left) vs. macrophages (right).

DISCUSSION & CONCLUSIONS: In conclusion, we have shown the fabrication of a 3D-printed co-culture platform, used a commercial biocompatible resin, and verified their utility in cultured epithelial cells and macrophages. Our initial results indicate monocyte differentiation in/on soft hydrogel substrates and culture intestinal barrier tissues on the 3D-printed platform; however, it is important to further verify this *via* immunostaining. Concurrently, the 2D and 3D microenvironment the effects will be investigated to elucidate the relationship between co-cultured cells.

ACKNOWLEDGEMENTS: This project has received funding from the European Union's Horizon 2020 research and innovation program under the Marie Skłodowska-Curie grant agreement No. 812673 and was conducted within the Organoids for Virus Research (OrganoVIR) network.

REFERENCES: [1] Bain and Schridde, *Frontiers in Immunology*, **2018**, v. 9, p. 2733; [2] Jepsen et al., *Advanced Biosystems*, **2020**, 1900289.

Tailoring the Printability of Methacrylated Gellan Gum Biomaterial Ink for Extrusion-based 3D Bioprinting

H. Jongprasitkul¹, S. Turunen^{1,2}, V.S. Parihar¹, M. Kellomäki¹

¹Biomaterials and Tissue Engineering Group, BioMediTech, Faculty of Medicine and Health Technology, Tampere University, Tampere, Finland, ²Brinter Limited, Turku, Finland

INTRODUCTION: Recently, photocross-linkable bionics are becoming popular choices in 3D bioprinting due to their versatility and ease of use [1]. Methacrylated gellan gum (GGMA) precursor has been proven to possess good rheological properties for an injectable hydrogel due to its inherent viscosity [2]. Unfortunately, the GGMA precursors alone are unable to maintain a stable filament shape when extruded from a nozzle.

METHODS: Two-step crosslinking technique involving ionic and photocrosslinking changed a GGMA ink printable. In the presence of an ionic crosslinker (Ca^{2+}), GGMA transformed from a liquid precursor to a weak extrudable hydrogel followed by photocrosslinking at 365 nm turning a weak hydrogel into a true hydrogel with good shape fidelity. The printability of various GGMA ink compositions (1, 2 and 3% GGMA with 22.5, 45 and 90 mM CaCl_2) was prescreened by characterising the rheological properties. A quantitative approach was introduced to quantify the experimental printability of different GGMA/ CaCl_2 ink compositions from the printed two-layered grid structures and 3D cylinders.

RESULTS: 2% GGMA with 90 mM CaCl_2 as a pre-crosslinker provided the best printability. The optimum ink formulation was then used to print 3D cylinders; which dimensions were then compared to the dimensions of the control material (Nivea crème) (Fig. 1). This optimised GGMA ink provided high printability ($Pr = 0.97$) during the fabrication (Fig. 2).

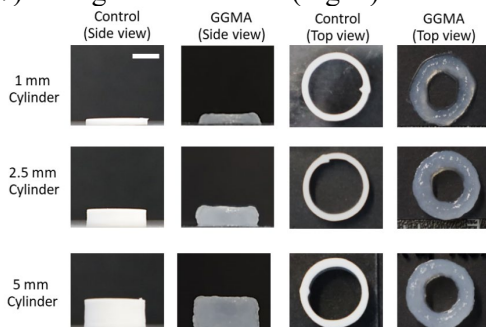


Fig. 1: The multi-view of printed cylinders for the evaluation of printing accuracy. The scale bar = 5 mm.

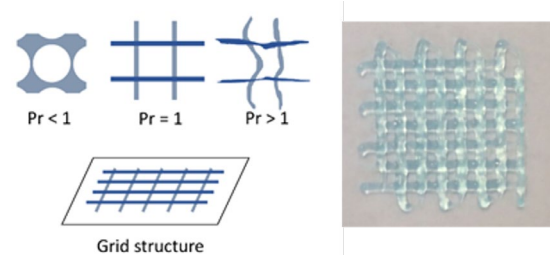


Fig. 2: The calculation of the printability (Pr) value. $Pr = 1$, indicating perfectly square-shaped pores.

DISCUSSION & CONCLUSIONS: The pre-crosslinking technique was developed to convert low viscous GGMA ink into an extrudable hydrogel with sufficient stackability to form 3D constructs before photocrosslinking. These cylinders presented high accuracy, shape fidelity, structural integrity and mechanical stability.

ACKNOWLEDGEMENTS: The authors are grateful to The Centre of Excellence in Body-on-Chip Research (CoEBoC) by the Academy of Finland and to the Tampere University funding for CoEBoC.

REFERENCES: [1] K.S. Lim et al, Chem. Rev., 2020, v. 120(19), p. 10662; [2] T.M. Robinson et al., ACS Biomater. Sci. Eng., 2020, v. 6(6), p. 3638.

Biodegradable Cross-linked Composite Hydrogels Based on Natural Components and Akermanite Enriched with Small Molecules for Osteochondral Regeneration

E.I. Oprita¹, T. Ciucan¹, A.M. Seciu-Grama¹, R. Tatia¹, R. Barabas², O.C. Raduly-Fazakas³, A.M. Gheorghe¹, O. Craciunescu¹

¹National Institute R&D for Biological Sciences, Bucharest, RO, ²Babeş-Bolyai University, Cluj-Napoca, RO, ³Chemi Ceramic F LTD, Sfântu Gheorghe, Covasna, RO

INTRODUCTION: The current study has developed variants of biodegradable cross-linked composite hydrogels based on natural polypeptides (gelatin), polysaccharidic components (chondroitin-4-sulphate and hyaluronic acid), mixed with akermanite and enriched with small bioactive molecules (icariin). Akermanite was used as better alternative to conventional ceramics, due to its bone-like apatite formation ability and good bioactivity [1]. Icariin (Ica) flavonoid (from traditional Chinese medicine *Epimedium* herb) was used as substitute for growth factors to enhance cell proliferation, chondrogenic and osteogenic differentiation [2].

METHODS: The biodegradable cross-linked composite hydrogels were prepared by mixing gelatin with two natural polysaccharidic components (chondroitin-4-sulphate and hyaluronic acid) in a ratio of 1:0.04:0.01 (w/w/w) (var. 1) and 1:0.4:0.01 (w/w/w) (var. 2). Then, the natural mixture variants were combined with akermanite in a ratio of 1:1 (w/w). Subsequently, both composite hydrogel variants (H1 and H2) were cross-linked with (N, N-(3-dimethylaminopropyl)-N-ethyl carbodiimide (EDC) and enriched with small bioactive molecule (Ica). The obtained composite hydrogel variants were characterized for their physicochemical properties in terms of the enzymatic biodegradation (in the presence of collagenase), swelling capacity, degree of cross-linking (TNBS assay) and morphology (SEM). Their cytocompatibility was evaluated by analyses of cell viability and cellular cycle (flow cytometry), cell proliferation (Neutral Red assay) and cell adhesion to composite hydrogels (SEM) using NCTC clone L929 cell line.

RESULTS: The results showed that the values of physicochemical characteristics varied depending on the composition and the degree of cross-linking of hydrogels. The degree of

swelling was influenced by the polysaccharide amount present in the composition of hydrogels. In addition, it was observed that an increase of the cross-linking degree led to a decrease of the swelling degree for both hydrogel variants, compared to non-cross-linked control. EDC cross-linked hydrogels also showed a controlled biodegradability in the first 6 h of incubation with collagenase, compared to the non-cross-linked variants. At 24 h of incubation in the presence of collagenase, all hydrogel variants were degraded. Cross-linked composite hydrogel variants (H1 and H2) were non-cytotoxic. It was observed the high cell viability in NCTC stabilized cell line within the tested range of concentrations (10 – 50 mg/mL) after 48 and 72 h of incubation. Moreover, cells were capable of spreading and proliferating on both composite hydrogel surfaces after 24 h.

DISCUSSION & CONCLUSIONS: Both cross-linked composite hydrogel variants (H1 and H2), enriched with Ica, presented optimal physicochemical, structural and biological properties to be used as a natural scaffold, able to repair osteochondral defects. The designed biodegradable cross-linked composites enriched with Ica are recommended for further testing as natural temporary scaffolds, which can allow cell migration and synthesis of new extracellular matrix within osteochondral defects.

ACKNOWLEDGEMENT: This work was supported by the grant of the Ministry of Research, Innovation and Digitization, CNCS/CCCDI – UEFISCDI, project number PN-III-P2-2.1-PED-2019-1714, within PNCDI III.

REFERENCES: [1]. P. Morouço et al., J. Funct. Biomater., **2021**, v. 12(1), p. 17; [2]. N. Goonoo et al., RSC Adv., **2019**, v. 9, 18124.

Study on the Effect of Fibrin Matrice on the Antibacterial Activity of Clindamycin Phosphate

K. Egle^{1,4}, L. Micko^{2,3,4}, A. Grava^{1,4}, I. Salma^{2,3,4}, I. Skadins^{4,5}, A. Dubnika^{1,4}

¹Rudolfs Cimmins Riga Biomaterials Innovations and Development Centre of RTU, Institute of General Chemical Engineering, Faculty of Materials Science and Applied Chemistry, Riga Technical University, LV, ²Institute of Stomatology, Riga Stradins University, LV, ³Department of Oral and Maxillofacial Surgery, Riga Stradins University, LV, ⁴Baltic Biomaterials Centre of Excellence, Headquarters at Riga Technical University, LV, ⁵Department of Biology and Microbiology, Riga Stradins University, LV

INTRODUCTION: Platelet-rich fibrin (PRF) is an autologous material derived from a person's own blood, which is used to promote wound healing and tissue regeneration [1]. Clindamycin phosphate (CLP) is a semi-synthetic bacteriostatic lincomycin derivative with activity against anaerobic bacteria [2]. Combination of PRF and CLP may enhance their antibacterial properties. The aim of this study was to investigate the effect of PRF on the antibacterial efficacy of clindamycin phosphate against *Staphylococcus aureus* and *Staphylococcus epidermidis*.

MATERIALS & METHODS: Written consent from all three volunteers for use of their samples in the research studies was obtained. Permission No. 6-2/10/53 of the Research Ethics Committee of Riga Stradins University has been received for the research.

A. Preparation of the PRF

Blood from healthy volunteers was collected and centrifuged at 700 rpm, 5 min for women, 6 min for men. Followed by separation of PRF by automatic pipette.

B. Antibacterial tests with microdilution method

S.aureus and *S.epidermidis* solutions were prepared according to EUCAST standards. CLP powder form was mixed with Mueller-Hinton Broth (MHB) and PRF in 2 different ways. In the first case, MHB was added first and then PRF (CLP/MHB/PRF_1). In the second case, PRF was added to CLP and then the MHB was added (CLP/MHB/PRF_2). The PRF/MHB ratios of 1:9 and 2:8 were used in the experiment. The resulting CLP / MHB / PRF solution was transferred to a 96-well plate and diluted from 1000 µg/mL to 7.81 µg/mL. A bacterial suspension was added on top. 96-well plates were incubated for 24 hours in 37°C.

After 24 hours, antibacterial effect was measured using microplate reader. In addition,

the kinetics of CLP release by ultra-performance liquid chromatography (UPLC) and the chemical structure by Fourier transform infrared spectroscopy (FTIR) were determined for the samples.

RESULTS: The order in which the PRF and broth are combined with the CLP solution is irrelevant. In turn, increasing the ratio of PRF (2:8) results in a greater difference in minimum inhibitory concentration (MIC) between pure CLP solution and CLP / PRF solution against both bacteria.

Table 1. MIC of CLP and CLP/PRF against test microorganisms, µg/mL.

Bacteria	<i>S.aureus</i> , MIC µg/mL	<i>S.epidermidis</i> , MIC µg/mL
CLP	125	125
CLP/MHB/PRF_1 1:9 (PRF:MHB)	62.5	62.5
CLP/MHB/PRF_2 1:9 (PRF:MHB)	62.5	125
CLP/MHB/PRF_1 2:8 (PRF:MHB)	31.25	62.5

DISCUSSION & CONCLUSIONS: The CLP/MHB/PRF solution shows better antibacterial results. In addition, no coagulation of the samples in the bacterial suspension was observed.

ACKNOWLEDGEMENTS: This research was funded by the European Union's Horizon 2020 research and innovation programme under the grant agreement No 857287 and the Latvian Council of Science research project No. lzp-2020/1-0054 (MATRI-X)".

REFERENCES: [1] E. Anitua et al., Trends Biotechnol., 2006, v. 24, p. 227; [2] R.R. Resnik et al. Elsevier, 2018; p. 294.

Calcium Phosphate Bone Cements for Anticancer Drug Delivery

A. Pylostomou^{1,2}, D. Loca^{1,2}

¹*Rudolfs Cimdins Riga Biomaterials Innovations and Development Centre of RTU, Institute of General Chemical Engineering, Faculty of Materials Science and Applied Chemistry, Riga Technical University, Riga, LV,* ²*Baltic Biomaterials Centre of Excellence, Headquarters at Riga Technical University, Riga, LV*

INTRODUCTION: Bone cancer is a common metastatic cancer and it is traditionally treated by surgery, chemotherapy or radiotherapy [1]. However, these methods exhibit several drawbacks, including the possibility of cancer re-emergence, inflammation and systemic toxicity, especially when chemotherapeutic drugs are administered orally or intravenously [2]. Therefore, alternative therapies where drugs could be delivered locally and in a well-controlled way are of clinical importance. Calcium phosphate bone cements (CPC) are suitable biomaterials for bone healing and regeneration, due to their biocompatibility and injectability. Moreover, their porosity facilitates the drug incorporation and release, making them suitable for drug delivery [3]. In this study, we developed α -TCP bone cements loaded with antineoplastic drug doxorubicin (DOX) and influence of liquid phase molarity on CPC/DOX setting time, mechanical properties, morphology, phase composition and drug release kinetics was evaluated.

METHODS: The final setting time of all CPC compositions was determined at 21 °C using the standard Vicat needle method. The compressive strength was measured at a loading rate of 0.5 mm*min⁻¹ using universal testing machine (INSTRON 10 kN, Norwood, MA). The morphology and microstructure of CPC were examined by scanning electron microscopy (SEM, Mira/LMU, Tescan, Brno, Czech Republic). X-ray powder diffractometry (XRD, PANalytical X'Pert PRO, Westborough, MA) was used to analyse the phase composition of the samples. For the determination of DOX release kinetics, four replicate CPC/DOX samples were prepared, immersed in 3.5 mL of phosphate buffered saline (PBS) and incubated at 37 °C \pm 0.5 °C and 50 rpm (Environmental Shaker - incubator ES-20, Biosan, Riga, Latvia). PBS solution was taken directly from the vessels after 1h, 4h, 24h, 48h, 72h, 6d, 7d, 14d and 21d. The volume taken was replaced with fresh

PBS, keeping the total dissolution medium volume constant. DOX content in PBS was determined using ultraviolet-visible spectroscopy (UV/VIS spectrophotometer Evolution 300, Thermo Scientific, Waltham, MA) at λ = 480 nm.

RESULTS: Obtained results clearly showed that the drug entrapment increased the cement setting time for 20% (from 40 \pm 2 min up to 50 \pm 2 min), while no significant differences in compression strength values were observed. Furthermore, the obtained results have demonstrated the influence of liquid phase molarity on cement setting time and DOX release. Decrease of the salt solution molarity by 2 times led to the setting time increase from 25 \pm 2 min to 50 \pm 2 min. Similar trend was also observed for DOX release kinetics and the decrease of salt solution molarity resulted in increase of DOX cumulative release rate (from 6.43 \pm 0.19% to 9.62 \pm 0.59% after 21st day of experiment).

DISCUSSION & CONCLUSIONS: Obtained results clearly demonstrated the influence of liquid phase molarity on CPC/DOX setting time and drug release profiles. Although developed CPC/DOX combinations can gradually release the active substance within the prolonged period of time, CPC/DOX composite *in vitro* biocompatibility should be verified in future experiments.

ACKNOWLEDGEMENTS: This project has received funding from the European Union's Horizon 2020 research and innovation program under grant agreement No 857287 (BBCE).

REFERENCES: [1] E. Dickens et al., Surgery (Oxford), **2018**, v. 36(3), p. 134; [2] Eguia A, et al., Med Oral Patol Oral Cir Bucal., **2020**, v. 25(1), e71–83; [3] A.M. Yousefi, J Appl Biomater Funct Mater., **2019**, v. 17(4).

Levan Based Hydrogels for Biomedical Applications

M. Erginer Haskoylu¹, O. Kirtel¹, E. Toksoy Oner¹

¹*IBSB, Industrial Biotechnology and Systems Biology Research Group, Marmara University, Department of Bioengineering, Istanbul, TR*

INTRODUCTION: Biopolymers are highly preferred in hydrogel synthesis with their cell surface interaction, physiochemical compositions, rheological and biological properties like biocompatibility, anticancer and antimicrobial activities [1, 2]. Levan is a homopolysaccharide of β (2 \rightarrow 6) – linked fructose units and this fructan biopolymer is produced by various microorganisms and plants. Our research group is mainly focused on this polymer to enlighten its potential to be used in different biomaterial studies including hydrogels with its water soluble, film former, nontoxic, biocompatible, and strongly adhesive features. Halomonas levan (HL) is produced by halophilic *Halomonas smyrnensis* bacteria with high yields from sucrose as a substrate. Among microbial levan producers, this extremophilic production system brings advantages like enabling unsterile and low-cost production. In recent years, heparin-mimetic material, nano and micro drug carrier systems, adhesive multilayer and blend films, laser deposited surfaces, electrosprayed nanoparticles for resveratrol releaser and temperature responsive hydrogels of HL were studied [1]. Recently, HL and its chemically modified forms crosslinked via 1,4-butanediol diglycidyl ether (BDDE) are being synthesized to develop adhesive hydrogels with amphotericin B [3] and resveratrol [3] release for dermal local antifungal therapy of Candidiasis and wound healing applications.

METHODS: Microbial levan (HL) was produced by *H. smyrnensis* and molecular weight is reduced (hHL) and phosphonated (PhHL). HL and derivatives were crosslinked with BDDE in different concentrations and characterized. Swelling ratios of the hydrogels were investigated together with their resveratrol and amphotericin B release kinetics and biocompatibility on human keratinocyte (HaCaT) and murine fibroblast (L929) cell lines *in-vitro* [1,3].

RESULTS: High swelling ratios (9.1 ± 0.1) of hydrogels synthesized with HL (1:2 BDDE: HL) were observed. Release of loaded AmB was recorded as 51% into PBS (2h) and strong

antifungal activity against *Candida albicans* was recorded with high biocompatibility with L929 murine fibroblast cell line. HL20 hydrogels (1:20) showed 5.095 ± 0.15 swelling in PBS at 37°C and almost all hydrogels showed high amount of resveratrol release within 6 hours. Increasing shear stress levels and superior adhesive properties of PhHL hydrogels were observed from track test analysis. High cell viability was observed for all hydrogels, but PhHL hydrogels showed greater cell proliferation ability when compared with others.

DISCUSSION & CONCLUSIONS: Obtained results pointed to the high potential of the gels for skin tissue engineering and drug delivery purposes. In the light of these studies, further studies for wound healing patches with active ingredient releasing or stem cell encapsulated injectable dermal fillers can be pursued using the enhanced adhesive, hydrophilic, controlled swelling, drug releasing and cell proliferation supporting properties of these hydrogels. Also, there are high potentials for these hydrogels to be used in pharmaceutical and cosmetic industries, which in turn need to be investigated.

ACKNOWLEDGEMENTS: Special thanks to INJECT-BIO project and 119N756 project for financial support.

REFERENCES: [1] S.S. Selvi et al., Journal of Bioactive and Compatible Polymers, **2021**, v. 36(6), p. 464; [2] E. Toksoy Öner et al., Biotechnology Advances, **2016**, v. 34, p. 827-844; [3] T. Demirci et al., European Journal of Pharmaceutical Sciences, **2020**, v. 145, 105255.

Fabrication and Characterization of Tricalcium Phosphate (TCP) Scaffolds Using the Foam Replica Method

S. Skibiński¹, E. Cichoń¹, P. Pańtak¹, J. P. Czechowska¹, A. Śłosarczyk¹, A. Zima¹

¹Faculty of Materials Science and Ceramics, AGH University of Science and Technology, Krakow, Poland

INTRODUCTION: The development of scaffolds for bone tissue engineering is a constantly growing field of medicine. Therefore, there is a continuous need for creating materials that possess appropriate physicochemical properties such as adequate phase composition and microstructure, open porosity and sufficient mechanical strength. Due to the high biocompatibility and bioactivity of tricalcium phosphates (α -TCP, β -TCP), they are one of the most commonly used bone substitutes. Foam replica method has been widely applied as a valuable technique for the fabrication of porous bioceramic materials with three-dimensional, open-cell microstructure mimicking human cancellous bone [1,2]. This work presents the properties of TCP-based scaffolds, evaluated in relation to processing parameters and sintering conditions.

METHODS: In our study, tricalcium phosphate-based scaffolds were prepared by a foam replication method. The use of different polyurethane matrices and various amounts of the solid phase (β -TCP powder) per volume of polymeric sponges enabled to obtain materials with distinct physicochemical features. Furthermore, the influence of sintering conditions (1100, 1150, 1200 and 1250 °C) on the materials properties was examined. Obtained materials have been investigated by various techniques such as powder X-ray diffraction, scanning electron microscopy, hydrostatic weighing, compression tests and chemical stability tests *in vitro* in simulated body fluid.

RESULTS: It was found that the microstructure of bioceramic scaffolds was characterised by a network of interconnected spherical pores with sizes between ~100 to ~1000 μm (Fig. 1). Obtained materials possessed open porosity in the range of about 56 to 70 vol% and compressive strength between 2.4 ± 0.7 and 4.8 ± 1.0 MPa. XRD analysis revealed that the materials sintered at 1100 °C, 1150 °C consist of one crystalline

Phase – β -TCP, while ones sintered at 1200 °C and 1250 °C consist of two crystalline phases: β -TCP (98 ± 1 wt% and 89 ± 1 wt%) and α -TCP (2 ± 1 wt% and 11 ± 1 wt%), respectively. Changes in the microstructure were observed in terms of grains shape and size. In the case of samples sintered at 1200 °C and 1250 °C the microcracks, caused by the volume change occurring during the β -TCP \leftrightarrow α -TCP phase transformation, were observed. The simulated body fluid immersion test proved that all scaffolds were chemically stable.

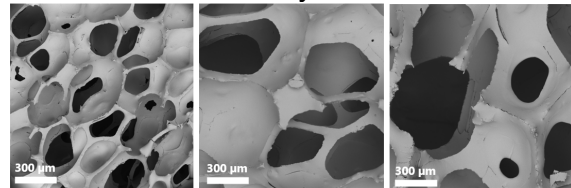


Fig. 1: Microstructure of the scaffolds depending on the type of polyurethane matrices used.

DISCUSSION & CONCLUSIONS: This study shows that foam replica technique is a relatively simple and effective method of obtaining TCP-based scaffolds with distinct physicochemical properties. Porosity and compressive strength can be adjusted by using different polyurethane matrices and amounts of solid phase (β -TCP powder) per volume of polymeric sponges. The monophasic β -TCP scaffolds, sintered at 1150 °C, were found to be the most favourable in the terms of material microstructure and mechanical strength.

ACKNOWLEDGEMENTS: Research funded by the National Centre for Research and Development, Poland, grant Techmatstrateg no. TECHMATSTRATEG2/407507/1/NCBR/2019

REFERENCES: [1] Fiume, et al., *Materials*, **2021**, v. 14(11), 2795; [2] Skibiński et al., *Ceramics International*, **2021**, v. 47(3), p. 3876.

Silver Decorated β -TCP Scaffolds for Bone Tissue Regeneration

J.P. Czechowska¹, S. Skibiński¹, E. Cichoń¹, P. Pańtak¹, A. Ślosarczyk¹, A. Zima¹

¹Faculty of Materials Science and Ceramics, AGH University of Science and Technology, Krakow, Poland

INTRODUCTION: Surgical procedures in orthopaedics are associated with a high risk of bacterial infections leading to postoperative complications. Therefore, biomaterials based on calcium phosphates enriched with antibacterial agents, such as antibiotics or bactericidal ions have been intensively studied [1,2]. The presence of silver in β tricalcium phosphates (β -TCP) may confer antibacterial properties, as this element exhibits a broad spectrum of antimicrobial activity against both gram-positive as well as gram-negative bacteria. Thus, the aim of this study was to obtain and characterize scaffolds based on silver-modified β tricalcium phosphate (Ag- β TCP).

METHODS: Silver modified β tricalcium phosphate (Ag- β TCP) powder was prepared by the precipitation method, using phosphoric acid, $\text{Ca}(\text{OH})_2$ and silver nitrate as the substrates. The amount of silver was equal 1.0 wt.%. Precipitate was left to mature, centrifuged, dried, calcined at 900 °C, grounded in an attritor mill and sieved (below 63 μm). Scaffolds were obtained using the foam replication technique. Polyurethane templates were immersed in ceramic slurry composed of Ag- β TCP powder, distilled water, Dispex A4040 and methylcellulose. Then specimens were dried and sintered at 1150 or 1200°C. The phase composition of the initial powder was analyzed via the High-Temperature X-Ray Diffraction (HT-XRD) and the phase composition of scaffolds was analyzed via the powder X-ray diffraction method. X-ray fluorescence method (XRF) was applied to determine the chemical composition of the obtained materials. The microstructure of scaffolds was assessed using scanning electron microscopy (SEM-EDS), porosity by hydrostatic weighing and compressive strength via universal testing machine Instron.

RESULTS: HT-XRD analysis of the non-calcinated Ag- β TCP powder showed that between 25°C and 300°C it consists of calcium-deficient hydroxyapatite (CDHA) and when calcined above 800°C (up to 1200 °C) transforms into crystalline β TCP. XRD studies showed that scaffolds sintered at 1150 and

1200 °C composed of only one crystalline phase *i.e.* β TCP. The incorporation of silver in the materials was confirmed by XRF and SEM-EDS studies. Silver particles of sizes between 624 ± 139 nm and 199 ± 37 nm were observed on the surfaces of scaffolds after sintering at 1200 and 1150 °C, respectively (Fig. 1).

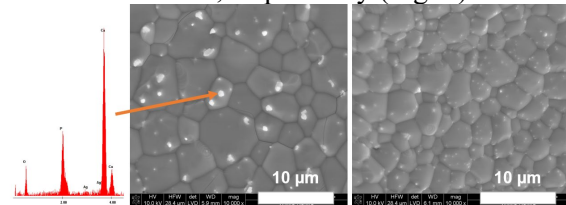


Fig. 1: Microstructure of the Ag- β TCP scaffolds sintered at 1200 (left) and 1150 °C (right).

The obtained materials possessed total porosity of around 70 vol% with the spherical pores between 100 and 700 μm . Ag- β TCP scaffolds sintered at 1200 °C (2.1 ± 0.6 MPa) possessed lower compressive strength than those sintered at 1150 °C (3.1 ± 0.6 MPa).

DISCUSSION & CONCLUSIONS: The macroporous β tricalcium phosphate scaffolds modified with silver (Ag- β TCP) were successfully obtained using the polyurethane foam replica method. The scaffolds sintered at 1150 °C, were found to be the most promising. Sintering in higher temperatures resulted in regions with intergranular microcracks. Further physicochemical and biological studies are needed to fully characterize developed biomaterials.

ACKNOWLEDGEMENTS: Research funded by the National Centre for Research and Development, Poland, grant Techmatstrateg no. TECHMATSTRATEG2/407507/1/NCBR/2019

REFERENCES: [1] Chou, et al., *Ceramics International*, **2020**, v. *46(10)*, p. 16708; [2] Siek et al., *Ceramics International*, **2017**, v. *43(16)*, p. 13997.

Short and Medium Chain Length Polyhydroxyalkanoates as Coatings of β Tricalcium Phosphate Scaffolds for Bone Tissue Regeneration

P. Pańtak¹, S. Skibiński¹, J.P. Czechowska¹, E. Cichoń¹, M. Guzik², A. Ślosarczyk¹, A. Zima¹

¹Faculty of Materials Science and Ceramics, AGH University of Science and Technology, Krakow, Poland, ²Jerzy Haber Institute of Catalysis and Surface Chemistry Polish Academy of Sciences, Krakow, Poland

INTRODUCTION: Scaffolds based on β tricalcium phosphate (β -TCP), due to their outstanding biocompatibility and bioactivity, are commonly used as bone substitutes. However, porous bioceramics demonstrate low compressive strength and high brittleness. An efficient approach to improve the mechanical properties of fragile scaffolds is to cover them with biocompatible and biodegradable polymers. Wide range of synthetic and natural polymers such as polycaprolactone, gelatin, collagen, silk or chitosan have been applied for this purpose [1]. The polyhydroxyalkanoates (PHAs) are green alternatives to conventional polymers and have been mostly used in soft tissue regeneration. These biocompatible and bioresorbable polymers depending on the polymer chain structure, differ in their physicochemical and mechanical properties. In this work, short chain length poly(3-hydroxybutyrate) (PHB) and medium chain length polyhydroxyoctanoate (PHO) were proposed as coatings of β tricalcium phosphate scaffolds. The influence of the polymeric coating on the microstructure, porosity, and compressive strength of the obtained materials was determined.

METHODS: Firstly, β -TCP scaffolds were obtained by the foam replication method. The polyurethane foams were impregnated in the slurry composed of β -TCP powder, distilled water, Dispex A4040, and methylcellulose, dried and sintered at 1150 °C. Next, obtained bioceramic scaffolds were immersed in the PHB or PHO solutions, dried and left for 7 days to solvent evaporation. Non-coated and composite scaffolds were characterised by X-ray diffraction method, scanning electron microscopy, hydrostatic weighing and compression test.

RESULTS: XRD and SEM studies confirmed the presence of polymeric layers on β -TCP scaffolds. However, PHB coating possessed microporous surface in contrast to smooth PHN layer. The total porosity of the non-coated and

composite scaffolds was similar and equal c.a. 70 %vol. Composites possessed higher compressive strength (TCP/PHB: 4.5 ± 0.5 MPa; TCP/PHO: 5.2 ± 0.9 MPa) when compared to non-coated materials (TCP: 3.7 ± 0.9 MPa). SEM observations after mechanical test (Fig. 1) revealed the presence of polymeric microfilaments that combine ceramic cracks in composite scaffolds.

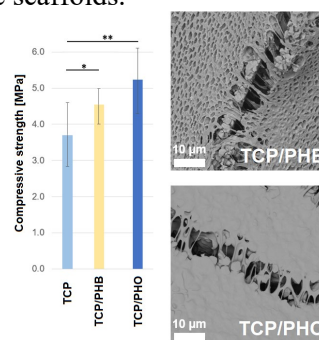


Fig. 1: Compressive strength of the obtained materials and microstructure of the composites after compression test.

DISCUSSION & CONCLUSIONS: Both, relatively brittle PHB and elastic PHO had a positive impact on mechanical behaviour of TCP scaffolds. Unlike the brittle bioceramic scaffolds, materials coated with polymers after compression maintained their integrity, which is a desirable feature for grafting materials. The difference in the microstructure of the polymer layers (microporous PHB and smooth PHO) may further affect the cell adhesion to the material surface. Therefore, additional biological *in vitro* studies are necessary.

ACKNOWLEDGEMENTS: Research funded by the National Centre for Research and Development, Poland, grant Techmatstrateg no. TECHMATSTRATEG2/407507/1/NCBR/2019

REFERENCES: [1] Gao et al., International journal of molecular sciences, 2014, v. 15(3), p. 4714.

Metabolomics Investigation of Biomaterial-Cell Interactions

J. Fan^{1,2}, T. Schiemer³, A. Sizovs^{2,4}, J. Locs^{1,2}, K. Klavins^{1,2}

¹*Rudolfs Cimdins Riga Biomaterials Innovations and Development Centre, Riga Technical University, Riga, Latvia;* ²*Baltic Biomaterials Centre of Excellence, Headquarters at Riga Technical University, Latvia;* ³*Medical University of Innsbruck, Innsbruck, Austria;* ⁴*Latvian Institute of Organic Synthesis, Riga, Latvia*

INTRODUCTION: The interaction between cells and materials is fundamental in biomaterial development. The scientific attention of biomaterial-cell interactions mainly falls on cell phenotype, protein, and nucleic acids, while the intracellular molecular mechanisms are often overlooked. Measuring metabolites directly can provide clues of cellular metabolism changes and help to explain and predict cell phenotype changes. The metabolism pathway changes can also be integrated with the data from assays, to increase understanding of cell physiological states. Detailed knowledge of the biomaterial-induced changes in cell metabolism is crucial for developing novel biomaterials-based therapeutic strategies and for creating in vitro test systems that significantly better predict in vivo risks and outcomes.

METHODS: In this study, calcium phosphates with different compositions were applied as the model material to investigate the cellular response. Specifically, hydroxyapatite (HAP), β -tricalcium phosphate (β -TCP), and bicalcium phosphate (BCP) were sintered into small discs. The calcium phosphate discs were characterized by XRD and then seeded with NIH/3T3 cells. Cells were harvested on days 1, 3, 5, and 7, following methanol-chloroform mixture extraction protocol to collect metabolites and lipids. Targeted quantitative metabolite analysis was carried out using HILIC based separation, combined with mass spectrometric detection, employing Thermo Orbitrap QExactive mass spectrometer.

RESULTS: Distinct changes in metabolite profiles for cells seeded on different biomaterials compared to controls were observed. Pathway analysis comparing metabolite profiles (between cells grown on HAP, β -TCP, and BCP for 24 hours and control cell culture) showed that metabolism and biosynthesis of several amino acids and lipids have been changed.

DISCUSSION & CONCLUSIONS: The obtained results demonstrated that different calcium phosphate compositions, as well as cell exposure time induced distinct changes in cellular metabolism. The observed changes in amino acid metabolism were in line with previously reported gene expression and protein activity data for selected materials. These results demonstrated the ability of metabolomics to identify the biomaterial chemical composition influence on cellular metabolism and its link to cell phenotype changes.

ACKNOWLEDGEMENTS: The authors acknowledge financial support from European Union's Horizon 2020 research and innovation programme under the Marie Skłodowska-Curie grant agreement No. 898858 and European Union's Horizon 2020 research and innovation programme under the grant agreement No. 857287.

Development of Novel PLA-based Materials for Bone Scaffolds

V.G. Eliasson¹, P. Prouilhac², N. Dethoor², S.N. Karlsdóttir¹, S. Brynjólfsson¹, G. Örlygsson³, C.-H. Ng⁴

¹Faculty of Industrial Engineering, Mechanical Engineering and Computer Science University of Iceland, Reykjavík, Iceland, ²Grenoble INP – Phelma, Grenoble, France, ³IceTec, Reykjavík, Iceland, ⁴Genís hf., Siglufjörður, Iceland

INTRODUCTION: Polylactic acid (PLA) is a widely used polymer in medical implants today [1]. PLA scaffolds produced by 3D printing is a promising concept for bone tissue engineering [2]. The aim of this study was to prepare a 3D printable filament containing calcium phosphate (CaP), as well as a design of the structure, 3D print of scaffold and characterize prototype scaffold implants from the prepared filament, with varying porosity and a minimum pore size of 300 μm , mimicking the characteristics and functions of cortical-cancellous bone structures.

METHODS: Commercial desktop filament extruder and fused deposition modeling (FDM) 3D printer were used to prepare the filaments and print the scaffolds. Filaments with varying CaP-content were prepared and characterized with SEM and x-ray μCT . Prototype parts were designed with three different porosities of 25%, 50% and 70%. Scaffolds with wall thicknesses as low as 200 μm were printed and the mechanical properties measured.

RESULTS: A homogeneous distribution of CaP particles in the PLA-matrix was observed, both in SEM and x-ray μCT (Fig. 1). The compressive strength of printed scaffolds, depending on composition, design and porosity, ranged from below 5 MPa to values between 40 and 45 MPa. In comparison to cancellous bone (1.5 MPa to 45 MPa), this is satisfactory but unacceptable when compared to cortical bone (90 MPa to 209 MPa).

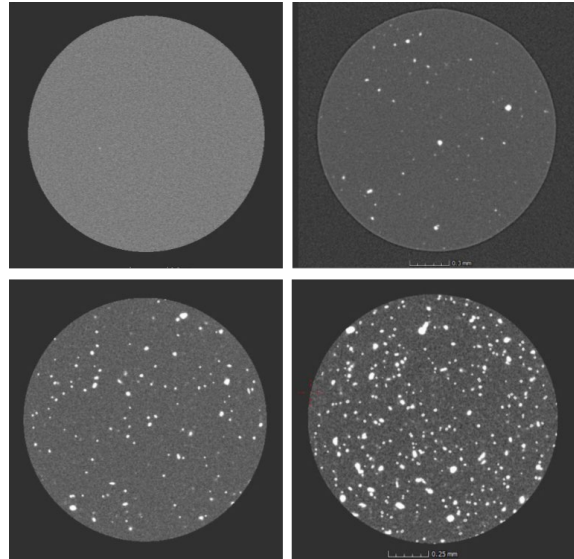


Fig. 1: Cross sections of prepared filaments. Top left: pure PLA, top right: 0.75%w/w CaP, bottom left: 1.5%w/w CaP, bottom right: 4.75% w/w CaP in filament.

DISCUSSION & CONCLUSIONS: The designs, production method and materials composition provide appropriate porosity, mechanical properties and biological conditions to allow cancellous bone tissue regeneration and could serve as a cost-effective way of creating regenerative implants for damaged or defective cancellous bone with an option of including bioactive components.

ACKNOWLEDGEMENTS: This project was supported by the Icelandic Technology Development Fund, managed by the Icelandic Centre for Research, grant number 2010912-0612.

REFERENCES: [1] D. da Silva et al., Chem. Eng. J., **2018**, v. 340, p. 9. [2] N. Söhnling et al., Materials, **2020**, v. 13, p. 1836.

Calcium Phosphate Nanoparticles as Potential Carriers for Nucleic Acid Vaccines

A. Maheshwari¹, F. Righetti¹, B. Henriques-Normark^{1,2}, G.A. Sotiriou¹

¹Department of Microbiology, Tumor and Cell Biology, Karolinska Institutet, Stockholm, Sweden, ²Clinical Microbiology, Karolinska University Hospital, Stockholm, Sweden

INTRODUCTION: Nucleic acid-based vaccines have potential for prevention of infectious diseases. However, these vaccine formulations suffer from poor immunogenicity and stability issues [1]. To tackle these problems, nanoparticles can be used as vaccine delivery platforms. Nanoparticles can protect the antigen cargo, improve immunogenicity, and allow for targeted delivery [2,3].

Calcium phosphate (CaP) nanoparticles are one of the most promising nanoparticle delivery agents being studied. They are biocompatible, biodegradable and have been shown to illicit immune response. Moreover, CaP has high affinity for DNA and used extensively for DNA transfection which makes them suitable for nucleic acid vaccines. Size is a critical factor for nanoparticle carriers as it determines the mode of cellular uptake by Antigen presenting cells (APCs) which consequently controls the gene expression for nucleic acid vaccines. In this study we synthesise various CaP nanoparticles and optimize their hydrodynamic size as well as DNA loading capacity [3,4].

METHODS: The nanoparticles were produced in a single step process using flame spray pyrolysis (FSP), which is a scalable technique. Brunauer-Emmett-Teller (BET) method and dynamic light scattering (DLS) were used to estimate the primary particle size and hydrodynamic size of nanoparticles, respectively. Enhanced green fluorescent protein (EGFP) encoding DNA was used to evaluate the loading capacity of the nanoparticles.

RESULTS: The CaP nanoparticles synthesized using FSP tend to agglomerate in suspensions. Their hydrodynamic size is greater than 500 nm, nevertheless they have high DNA loading capacity (Fig. 1). The CaP were further synthesized with varying silica content for surface stabilization. So, we investigate its effect on nanoparticle hydrodynamic size and nucleic acid loading capacity.

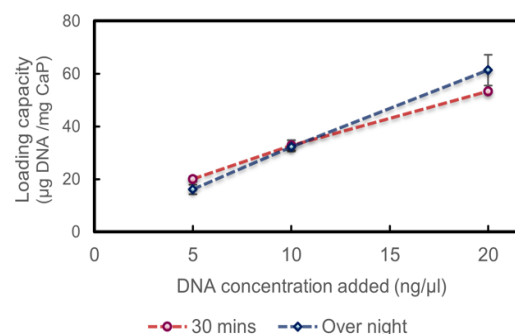


Fig. 1: Loading capacity of amorphous CaP nanoparticles for varying concentration of EGFP encoding DNA with 2 different incubation times- 30 mins (red) and overnight (blue).

DISCUSSION & CONCLUSIONS: We can use FSP to produce CaP nanoparticles and easily control their composition. Thus, we can optimize their hydrodynamic size while maintaining high nucleic acid loading capacity.

ACKNOWLEDGEMENTS: This research is funded by the Swedish Foundation for Strategic Research (FFL18-0043, RMX18-0041) and European Research Council (ERC) under the European Union's Horizon 2020 research and innovation program (ERC Grant agreement n° 758705). Funding from Karolinska Institutet Faculty Board, Swedish Research Council (2018-05798 and 2021-02059) is kindly acknowledged.

REFERENCES: [1] F. Qin et al., *Frontiers in cell and developmental biology*, **2021**, v. 9, p. 830; [2] A. Gutjahr et al., *Vaccines*, **2016**, v. 4(4), p. 34; [3] R. Pati et al., *Frontiers in immunology*, **2018**, v. 9, p. 2224; [4] Y. Lin et al., *Expert review of vaccines*, **2017**, v. 16(9), p. 895.

Bioactive Proteins Release Monitoring from 3D Printed Bone Scaffolds Prepared by Direct Ink Writing Technology

K. Lysáková¹, B. Přečková², K. Hlináková¹, P. Menčík^{1,2}, R. Příkryl^{1,2}, G. Örlygsson³,
C.H. Ng⁴, L. Vojtová¹

¹Brno University of Technology, CEITEC-Central European Institute of Technology, Advanced Biomaterials, Czech Republic, ²Brno University of Technology, Faculty of Chemistry, Czech Republic, ³IceTec, Reykjavík, Iceland, ⁴ Genís hf., Sigluffjörður, Iceland

INTRODUCTION: The problem with large bone defects is their slow healing, often accompanied by bone inflammation. The advantage of 3D robocasting over hand-processed or cast materials is mainly in setting the exact shape, size, and morphology of the final product. Calcium phosphate (CaP) ceramic powder modified with a thixotropic biodegradable thermosensitive copolymer (originally synthesized at CEITEC BUT [1]), and renewable biocompatible polysaccharide chitosan (developed by Genís hf.) were used as a resorbable bio-ink in this project. The low-temperature 3D printed bone scaffolds were enriched with bioactive proteins to accelerate the healing process along with suppressing microbial infection.

METHODS: Low-temperature 3D printed bone scaffolds prepared by direct ink writing technology were enriched with bioactive proteins in different ways (mixing with paste before printing or coating after printing). Subsequently, they were hardened differently in high humidity or aqueous environment. The protein was released into various environments (acidic, neutral, and alkaline) at body temperature. Protein release was monitored by a UV-VIS spectrophotometer in the presence of the Bradford reagent. Finally, the structure of the samples was monitored by scanning electron microscopy (SEM), and *in vitro* biological activity of the released protein was studied.

RESULTS: The model protein albumin was firstly used to set up the method. The way of incorporating the bioactive protein into the 3D printed bone scaffold has been found to play a key role. When bone cement was enriched with

protein before printing, no release was evident even after 30 days. When the protein was coated on a scaffold after the printing process and partial hardening in high humidity, protein release was observed. On the other hand, the hardening time of the bone carrier did not show a difference in the rate of protein release over time.

DISCUSSION & CONCLUSIONS: In this study, the release of bioactive proteins from 3D printed scaffolds and the influence of different factors (hardening, ways of protein incorporation) on the release rate and protein activity were observed. Since the whole printing process took place at room (ambient) temperature or at human body temperature (hardening of the final product) the biological activity of bioactive proteins was not affected. As has been shown, for bioactive substance-controlled release, more advantageous was to load the protein to the carrier (bone scaffold) after the 3D printing and hardening process. On the contrary, when the bioactive substance was mixed into the paste prior to printing, it led to a minimal protein release as a result of the protein tight incorporation into the structure of the bone scaffold over the hardening time thus protecting the protein-controlled release.

ACKNOWLEDGEMENTS: This work was supported by the ProfiBONE project (TO01000309) that benefits from the EEA Grants and the TACR within the KAPPA Programme.

REFERENCES: [1] L. Michlovská et al., *Macromol. Symp.*, **2010**, v. 295, p. 119.

Hydrogel Influence on Cell Metabolism

V. Jahedzomorodi^{1,2}, L.V. Kaufmane¹, F. Rastegar-Adib¹, K. Aunina¹, D. Loca^{1,2},
K. Klavins^{1,2}

¹Rudolfs Cimdins Riga Biomaterials Innovations and Development Centre, Riga Technical University, Riga, Latvia, ²Baltic Biomaterials Centre of Excellence, Headquarters at Riga Technical University, Riga, Latvia

INTRODUCTION: Hydrogels are hydrophilic biomaterials with 3D networks that enable uptake of biological fluids, providing a great candidate as a scaffold for cell localization in biomedical engineering. Although many *in vitro* tests have been proposed to evaluate the performance of the cells on/in hydrogels, still a comprehensive method is needed that elucidates the details of the intracellular molecular mechanism. Metabolomics, measurements of small endogenous molecules within a cell provide an efficient assessment to evaluate any changes in cellular behavior in response to an external signal. Recognizing metabolic perturbation of cells in contact with hydrogels could give accurate information about the behavior of cells/hydrogels *in vitro*, resulting in better translation of *in vivo* assay to clinical studies.

METHODS: Here, hyaluronic acid (HA) and polylysine (PL) polymers with different ratios will be physically cross-linked, resulting in high swellable *in situ* hydrogels. A targeted metabolomics study will be performed to evaluate the behavior of 3T3 fibroblast cells in exposure to the obtained hydrogel. In short, cells will be seeded directly onto the transwell plate, and a piece of hydrogel will be placed on the insert membrane. Cells will be harvested on days 1, 3, 5, and 7, following methanol-chloroform mixture extraction protocol to collect metabolites and lipids. Targeted quantitative metabolite analysis will be carried out using HILIC based separation combined with mass spectrometric detection employing Thermo Orbitrap QExactive mass spectrometer.

RESULTS: We have obtained the first results using HA/PL (70/30) hydrogels. Distinct changes in metabolite profiles for cells seeded on hydrogel compared to controls were observed. For example, levels of glutamic acid, alanine, aspartic acid, adenosine, glycine, etc., were significantly altered for the exposed cells (Fig. 1).

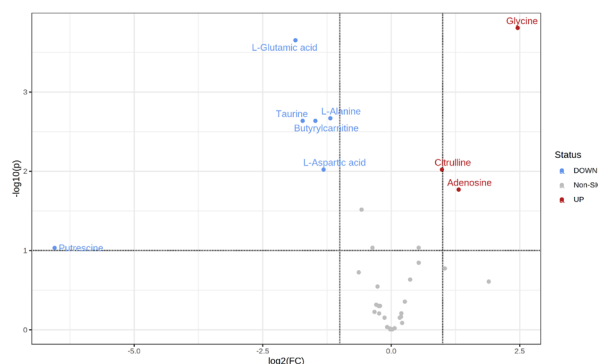


Fig. 1: Volcano plot depicting metabolite changes in cell metabolism upon exposure to HA/PL (70/30) hydrogel after 3 days.

DISCUSSION & CONCLUSIONS:

Preliminary results using HA/PL (70/30) hydrogel demonstrated that exposure to hydrogel causes a perturbation in several metabolic pathways such as arginine biosynthesis purine metabolism, and aminoacyl-tRNA biosynthesis. Interestingly, the results showed no significant change in media composition in the presence of hydrogel. The obtained results provide the fascinating first evidence that metabolite levels are changed by exposure to a hydrogel.

ACKNOWLEDGEMENTS: The authors acknowledge financial support from European Union's Horizon 2020 research and innovation programme under the Marie Skłodowska-Curie grant agreement No. 898858 and European Union's Horizon 2020 research and innovation programme under the grant agreement No. 857287.

The Potential of Latvian Honey for Antibacterial Biomaterial Improvements

A. Brangule^{1,2}, I. Skadiņš^{1,3}, J. Amirian^{1,2}, A. Mazurs^{1,2}, E. Pumpurs^{1,2}

¹Baltic Biomaterials Centre of Excellence, Headquarters at Riga Technical University, Riga,

LV, ²Riga Stradiņš University, Department of Pharmaceutical Chemistry, Riga, LV

³Department of Biology and Microbiology, Riga Stradiņš University, Riga, LV

INTRODUCTION: Honey is widely used in traditional medicine and modern wound healing biomaterial research as a broad-spectrum antimicrobial, anti-inflammatory and antioxidant agent. The natural properties, active compounds and physicochemical properties, such as the low pH (3.5–4) of honey, lower the alkaline medium of chronic wounds, stimulating wound healing. In addition, specific properties of honey can lead to the incorporation into biomaterials such as cryogels, hydrogels and bioactive glass. The study's objectives were to evaluate the antibacterial activity on Gram-positive and Gram-negative bacteria and their clinical isolates on monofloral honey samples collected from the beekeepers in the territory of Latvia.

METHODS: 40 different monofloral honey samples with known pollen concentrations were collected from the beekeepers in Latvia. The antimicrobial activity of Latvian honey samples was compared with commercial Manuka honey. To evaluate antibacterial properties of honey samples, reference cultures of *Staphylococcus aureus* (ATCC 25923), *Pseudomonas aeruginosa* (ATCC 14209), *Escherichia coli* (ATCC 25922) and antibiotic resistance clinical isolates of *Methicillin-resistant staphylococcus aureus* and *Extended Spectrum Beta-Lactamase (ESBL) producing Escherichia coli* were used in the study. Antifungal properties of honey samples were identified against the reference culture of *Candida albicans* (ATCC 10231). Antimicrobial activity was evaluated with the well diffusion method. Each honey sample dilution was prepared from an 80% honey solution (w/v). Microdilution methods were used to determine the Minimum Inhibitory Concentration (MIC) and Minimum Bactericidal Concentration (MBC) of the honey. Twofold serial dilutions of the compound solutions (ranging between 40% and 0.31%) were performed in 96 well plates (*SarsTEDT, Germany*).

RESULTS: Buckwheat and Clover honey samples exhibited a greater antibacterial effect on Gram-positive bacteria than other honey samples. The highest antibacterial activity was exhibited by Buckwheat (inhibition zone diameter 15.0–20.5 mm) and Clover (inhibition zone diameter 15–16 mm) honey samples against *Methicillin-resistant staphylococcus aureus*. Buckwheat and Manuka honey are equally effective on MRSA. Most samples exhibited a weak or moderate effect on Gram-negative bacteria.

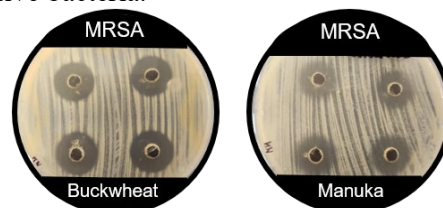


Fig. 1: Effect of Buckwheat and Manuka honey samples on *Methicillin-resistant Staphylococcus aureus*.

DISCUSSION & CONCLUSIONS: Buckwheat and Clover honey samples show excellent antibacterial activity against Gram-positive bacteria. Honey possesses some antimicrobial activity against the tested Gram-negative bacteria. Honey presents a promising potential to be used in wound healing biomaterials, therefore opening the possibility of achieving a long-term antibacterial effect.

ACKNOWLEDGEMENTS: This project has received funding from the European Union's Horizon 2020 research and innovation programme under the grant agreement No. 857287.

REFERENCES:

- [1] G. Bonsignore et al., "Green" Biomaterials: The Promising Role of Honey, **2021**; [2] 2. M. Arango-Ospina et al., Honey and Zein Coatings Impart Bioactive Glass Bone Tissue Scaffolds Antibacterial Properties and Superior Mechanical Properties, **2021**.

Eggshell-Derived Amorphous Calcium Phosphate and Low-Crystalline Apatite Ceramics

S. Zemjane^{1,2}, K. Rubenis^{1,2}, J. Locs^{1,2}, D. Loca^{1,2}

¹Rudolfs Cimdins Riga Biomaterials Innovations and Development Centre of RTU, Institute of General Chemical Engineering, Faculty of Materials Science and Applied Chemistry, Riga Technical University, Riga, Latvia, ²Baltic Biomaterials Centre of Excellence, Headquarters at Riga Technical University, Riga, Latvia.

INTRODUCTION: Chicken eggshell is a typical example of product-specific waste in the food industry. High content of calcium makes it an attractive precursor material for the synthesis of calcium phosphates that can be used in bone regeneration applications. So far, the use of chicken eggshells for the synthesis of amorphous calcium phosphate and low-crystalline apatite has received little attention. In the present study, we synthesized amorphous calcium phosphate and low-crystalline apatite by using eggshells as a source of Ca²⁺ ions and investigated the possibilities to densify the synthesized calcium phosphates by uniaxial compaction at room temperature.

METHODS: First, eggshells were calcined at 900 °C to obtain CaO. Then, CaO suspension in water was prepared, to which 4.76 M orthophosphoric acid was added. Afterwards, 3 M HCl was added to the synthesis solution to dissolve the precipitates. Finally, a 2 M NaOH aqueous solution was rapidly poured into the synthesis media to induce precipitation of the amorphous calcium phosphate. To produce low-crystalline apatite, the precipitate was left to stand in the synthesis solution for 24 h. The precipitates were collected by vacuum filtration, washed with deionized water and afterwards freeze-dried. Densification of the synthesized powders was done at pressures from 500 to 1500 MPa by automatic hydraulic laboratory press (pressing die with an inner diameter of 13 mm was used). The synthesized powders and the samples made from them were characterized by X-ray diffraction (XRD), Fourier transform infrared spectroscopy (FTIR), thermogravimetry (TG) and scanning electron microscopy (SEM). Additionally, their densities were determined.

RESULTS: XRD and FTIR confirmed that amorphous calcium phosphate and low-crystalline apatite was obtained. True density of the low-crystalline apatite was approximately 10 % higher than that of the amorphous calcium

phosphate while its water content was approximately 60 % lower. After densification, the samples retained amorphous calcium phosphate and low-crystalline apatite phase, however, changes were induced in their local structure. Both the amorphous calcium phosphate and low-crystalline apatite could be densified to a relative density >90 % by uniaxial compaction at 1500 MPa. The microstructure of the samples consisted of grain-like structure with grain sizes below 100 nm.



Fig.1: Photograph of the amorphous calcium phosphate ceramic sample obtained at 1500 MPa.

DISCUSSION & CONCLUSIONS: The results suggest that chicken eggshell can be used for the synthesis of highly stable amorphous calcium phosphate and low-crystalline apatite. Amorphous calcium phosphate and low-crystalline apatite can be sintered to a relative density >90 % by simple uniaxial compaction at 1500 MPa at room temperature.

ACKNOWLEDGEMENTS: The authors acknowledge financial support from the Baltic Research Programme project No. EEA-RESEARCH-85 “Waste-to-resource: eggshells as a source for next generation biomaterials for bone regeneration (EGGSHELL)” under the EEA Grant of Iceland, Liechtenstein and Norway No. EEZ/BPP/VIAA/2021/1.

Biomaterials and Blood Concentrates in Oral-Maxillofacial Surgery

A. Heselich¹, J. Smieszek², S. Ghanaati¹

¹ Goethe University, Clinic for Oral-, Maxillofacial and Plastic Surgery, FORM-lab, Frankfurt/Main, Germany, ² Department of Oral Surgery, School of Medicine with the Division of Dentistry in Zabrze, Medical University of Silesia in Katowice, Poland

INTRODUCTION: Regeneration of defects in the oral cavity can be challenging for the organism, even if only being small defects. One possibility to support the regeneration process is the use of biomaterials, for example bone substitute material for bone regeneration and/or membranes for soft tissue regeneration. Both can be used for the so-called guided bone or guided tissue regeneration (GBR/GTR). In this context biomaterials can serve as scaffolds to achieve a 3-dimensional structural support, as barrier to prevent early soft tissue infiltration and thereby disturbing bone regeneration, or as guidance for cell migration and penetration [1]. However, implantation of such synthetic, xenogeneic, allogenic, or even phylogenetic material can still bear some risk for unwanted cellular response, or material performance might be not sufficient enough for the intended use. A possibility for optimization is the biologization of such biomaterial, lacking any viable biological components due to the mandatory processing for use in clinical applications. Biologization can be easily achieved using autologous blood concentrates like platelet-rich fibrin (PRF), which is obtained by the centrifugation of patients own peripheral blood without any additional anticoagulants [2]. The development of systematic centrifugation protocols using the low-speed centrifugation concept (LSCC) allows the preparation of highly bioactive PRF matrices by the reduction of the applied centrifugal force during centrifugation [3]. The combination of any biomaterial with PRF matrices composed of platelets, leukocytes, plasma proteins, and growth factors stimulates the patient's self-regenerative capacity, by stimulating cell proliferation and migration from the surrounding tissue into the defect area. Further, the fibrinous structure of PRF can be a guidance for cellular migration. All supporting and even accelerating the bone and/or soft tissue regeneration.

METHODS: To better understand the effects of use of PRF in defect regeneration we started controlled randomized clinical trials with ridge

preservation defects following tooth extraction, thereby evaluating the effect on soft tissue wound healing and bone regeneration after treatment with different types of LSCC-PRF alone or in combination with bone substitute material (Fig. 1) compared to natural healing.

RESULTS: First evaluation of soft tissue regeneration already shows differences regarding use of PRF alone, or in combination with biomaterials, and further the efficacy depending on used biomaterial.

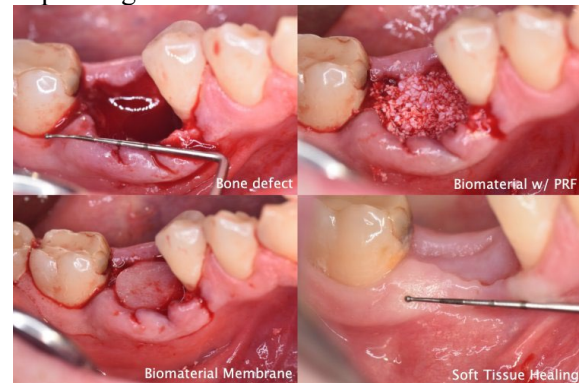


Fig. 1: Bone-substitute biomaterials and membranes in combination with autologous blood concentrate PRF in bone defect treatment (ridge preservation) after tooth extraction.

DISCUSSION & CONCLUSIONS: Early results indicating an influence of the chosen biomaterial – PRF combination emphasise the importance of understanding biomaterial characteristics for indication-specific use of biomaterials in clinical treatment.

ACKNOWLEDGEMENTS: The group is active member of the RISEus2 program (H2020, grand agreement No. 952347).

REFERENCES: [1] J. Lorenz, et al. *Ann Maxillofac Surg*, **2016**, v. 6(2), p. 175; [2] S. Al-Maawi et al., *Materials*, **2019**, v. 12(23), p. 17; [3] J. Choukroun, S. Ghanaati, *European Journal of Trauma and Emergency Surgery*, **2018**, v. 44(1) p. 87.

Lytic Activity of *Staphylococcus Aureus* Bacteriophages in Alginate Matrices

L. Stipniece^{1,2}, D. Rezevska³, D. Loca^{1,2}

¹Rudolfs Cimdins Riga Biomaterials Innovations and Development Centre, RTU, Riga, LV,

²Baltic Biomaterials Centre of Excellence, Headquarters at Riga Technical University, Riga, LV, ³Department of Biology and Microbiology, RSU, Riga, LV

INTRODUCTION: Bacteriophages are viruses that infect bacteria and use bacterial cells as sources for their replication [1]. Therefore, they are effective weapons against bacterial infections. However, bacteriophages have some disadvantages, such as low stability over time and low resistance (or short half-life) in highly acidic and alkaline environment. In order to maximize effectiveness of bacteriophages treatment, a carrier to reach the site of infection for specific application must be used. Moreover, careful consideration must be given to the physical and chemical parameters when choosing an immobilization method. To address this concern, employing controlled release entrapment platforms is of particular advantage. *S. aureus* is a major cause of various infections in humans and animals. *S. aureus* causes infections of the skin, soft tissues, bones and joints. Lytic bacteriophages of *S. aureus* have been used in the development of antibacterial materials [2]. This study evaluated the potential for bacteriophage immobilization in the alginate to control the release profile of the antimicrobials. Thus, the stability (*i.e.* maintenance of lytic activity) of *S. aureus* bacteriophages was assessed during various processing steps.

METHODS: Commercial bacteriophage cocktails (*Pyo* and *Staphylococcal*, Eliava BioPreparations Ltd.) were used to obtain *S. aureus* specific bacteriophage. 1 wt% Na-alginate solution with propagated lytic *S. aureus* bacteriophage solution (ratio 1:1) was prepared. Phage titer (PFU/mL) in the Na-alginate solution before and after drying, as well as after crosslinking with CaCl₂ was determined by a plaque assay using *S. aureus* reference strain ATCC 25923. In addition, the bacteriophages' titer in the TRIS-HCl after incubation of the bacteriophages containing Ca-alginate matrices was determined using the plaque assay.

RESULTS: *S. aureus* bacteriophages, namely, *Pyo* phage and *Staph* phage, showed good stability in Na-alginate solution with the titer

reduction of less than 1 log unit. It was observed that titer of the bacteriophages decreased during incubation at 40°C. No lytic zones (presence of the bacteriophages) were detected for the samples of completely dried Na-alginate. The titer reduction after cross-linking Na-alginate with CaCl₂ was below 1 log unit. In addition, titer of the bacteriophages embedded in Ca-alginate matrices remained reasonably close to the planned or nominal value $(2.1 \pm 0.2) \cdot 10^8$ PFU/mL.

DISCUSSION & CONCLUSIONS: Parameters and components for the development of polymer matrices containing lytic *S. aureus* bacteriophages were screened. The *S. aureus* bacteriophages retain their lytic activity in the Na-alginate solution. Drying of the Na-alginate matrices proved to be critical for loss of lytic activity of the bacteriophages. It was concluded that the most optimal option is to use the Ca-alginate matrices, where the embedded bacteriophages retain their lytic activity. After 72 h, only 0.29±0.02% of encapsulated bacteriophages were released from the Ca-alginate matrices. This suggests that such an approach can ensure a long-term local supply of bacteriophages.

ACKNOWLEDGEMENTS: This work has been supported by the ERDF within the Activity 1.1.1.2 "Post-doctoral Research Aid" of the Specific Aid Objective 1.1.1 "To increase the research and innovative capacity of scientific institutions of Latvia and the ability to attract external financing, investing in human resources and infrastructure" of the Operational Programme "Growth and Employment" (No. 1.1.1.2/VIAA/2/18/339). The authors acknowledge financial support from the European Union's Horizon 2020 research and innovation programme under the grant agreement No. 857287.

REFERENCES: [1] Qadir et al., Brazilian J Pharm Sci, **2018**; [2] Bachir et al., Battle Against Microb. Pathog. Basic Sci., **2015**.

Hydroxyapatite Nanoparticles with Strictly Controlled Particle Size for Bone Implants Coatings and Bone Filler Applications

U. Szalaj^{1,2}, J. Higuchi¹, K. Klimek³, G. Moczko⁴, A. Chodara¹, W. Łojkowski¹

¹Laboratory of Nanostructures, Institute of High Pressure Physics, Polish Academy of Sciences, Warsaw, Poland,; ²Faculty of Materials Engineering, Warsaw University of Technology, Warsaw, Poland, ³Department of Biochemistry and Biotechnology, Medical University of Lublin, Lublin, Poland, ⁴Syntropiq, Prague, Czech Republic

INTRODUCTION: Millions of bone reconstruction operations are conducted every year. A promising alternative to autologous bone grafts are customized bone scaffolds. Biofunctional custom implants fill the defect in the tissue and carry mechanical loads. The presence of groups with hydrophilic properties (e.g., -OH) on biomaterial surface is preferred. For this reason, the modification of the surface of polymeric and metal materials is becoming more and more popular. In the field of regenerative medicine, homogeneous, biocompatible, bioactive coatings stimulating the regeneration of bone or cartilage tissue. All these conditions are met by nano-hydroxyapatite layers deposited by sonocoating method. Hydroxyapatite (HAP) is the main mineral component of the bone, responsible for the stiffness and mechanical strength.

METHODS: GoHAP NPs were obtained using the hydrothermal microwave synthesis method described in detail by Kusnieruk et al. [1]. The fabricated nanoparticles were used in the process of coating the surfaces of titanium and polymeric implants by sonochemical method. The method of sonochemical deposition of hydroxyapatite layers was described by B. Wozniak, U. Szalaj, et al. [2] Three types of obtained nanoparticles, differing in particle size, were separately selected for coating: GoHAP with the particle size about 10 nm, 15 nm, 45 nm. As a control, commercial HA Biocer was used.

RESULTS: This work concerns a unique eco-friendly microwave synthesis process enabling strict size control of hydroxyapatite nanoparticles (GoHAPTM) in the range of 10±1 to 42±4 nm by controlling the synthesis parameters such as time, pressure and temperature. The complete characterization of GoHAPTM nanoparticles and the relationship between material properties and particle size has been demonstrated. This work presents the mechanism of formation of the nanoparticles

layer deposited by sonocoating, as well as the relationship between the size of nanoparticles used in the coating process and the properties of the deposited layer. The presentation shows the kinetics of the nanoparticles layer deposition process, depending on the GoHAP nanoparticles size, as well as the properties of the obtained layers, such as morphology or contact angle, biocompatibility.

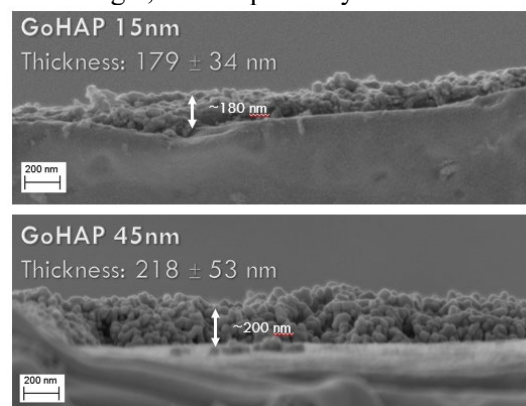


Fig. 1 Layer thickness investigations - SEM image analysis.

DISCUSSION & CONCLUSIONS: In case of hydroxyapatite nanoparticles, the particle size affects the efficiency of the sonocoating deposition process, as well as the properties of the hydroxyapatite layers. For this reason, special attention should be paid to the nanoparticle size in the design of new materials for bone tissue regeneration.

ACKNOWLEDGEMENTS: The following research was funded by the Centre for Preclinical Research and Technology -CePT II from the Operational Program of the Masovian Voivodship (RPMA.01.01.00-14-8476/17-01).

REFERENCES: [1] S. Kusnieruk, et al., Beilstein J. Nanotech., **2016**, v. 7, p. 1586; [2] B. Wozniak et al., Materials Letters, **2019**, v. 249, p. 155.

Advanced Characterization of Nanomaterials According to ISO Norm

A. Opalinska¹, U. Szalaj¹, E. Pietrzykowska¹, W. Lojkowski¹

¹Laboratory of Nanostructures, Institute of High Pressure Physics PAS Poland

INTRODUCTION: Characterization of nanomaterials is the key stage for technology process. Laboratory of Nanostructures is accredited by the Polish Centre for Accreditation and operates in accordance with ISO/IEC 17025:2005 „General requirements for the competence of testing and calibration laboratories”

METHODS: Our accredited methods: DLS method (Dynamic Light Scattering) Zetasizer Nano-ZS Malvern - measurement of particle size distributions; LDE method (Laser Doppler Electrophoresis) Zetasizer Nano-ZS Malvern zeta potential analysis; NTA method (Nanoparticles Tracking Analysis) - method of visualising and analysing particles in liquids, measurement of particle size distributions, Nanosight NS 500 and Viewsizer 3000; Density determination by helium, Specific surface area (SSA)

According to ISO standards we offer the following analysis:

Thermogravimetric analysis; Stability (MLS); X-ray Diffraction; Method for Chemical Composition - Chemical Analysis using SEM/EDS Surface analyses, chemical analysis and imaging on a variety of materials are performed using an Ultra Plus Zeiss. The SEM is equipped with an Energy Dispersive Spectrometer Quantax 400 Bruker.

RESULTS: Exemplary results of the nanoparticles size distribution are presented below

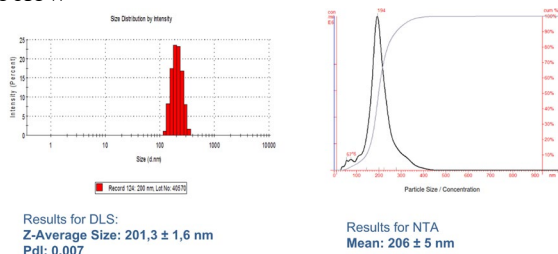


Fig. 1: Comparison of methods DLS and NTA on a monodisperse sample.

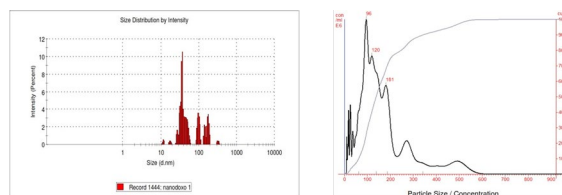


Fig. 2: Comparison of methods DLS and NTA on a polydisperse sample.

DISCUSSION & CONCLUSIONS: We have 20 years of experience in synthesis and characterization of nanoparticles and we understand well dependencies between nanoparticles properties and methods to synthesise nanoparticles as well quality issues.

ACKNOWLEDGEMENTS: The following research was funded by the Centre for Preclinical Research and Technology -CePT II from the Operational Program of the Masovian Voivodship (RPMA.01.01.00-14-8476/17-01).

Antifouling Coatings to Improve Implant Body Acceptance – a Model on Synthetic Polymer Meshes

E.D. Giol^{1,2}, D. Militaru¹, A. Dumitrascu², H. Iovu¹

¹ Politehnica University of Bucharest, Advanced Polymer Materials Group, Bucharest, Romania; ² 'Cantacuzino' National Medico-Military Institute for Research and Development, Bucharest, Romania

INTRODUCTION: An important obstacle during the implantation of a biomaterial is the activation of a “foreign body” reaction enabling a host-immune response, which is notably characterized by an inflammation and a fibrotic development around the implant. The deposition of an antifouling coating on biomaterials intended for implantation may act as a defensive line against host-immune reactions by preventing the adhesion of proteins and activation of platelets, limiting thus foreign body reaction and allowing the body to focus on healing. The antifouling behavior of poly(ethylene glycol) (PEG) and PEGylated derivatives has been valorized on the market for more than 20 years, resulting into their translation as vital ingredient in everyday products, surfactants and a series of medical applications. Nevertheless, various reports have shown that PEGylated products can cause immunological response, hypersensitivity or antibody generation [1-3]. Zwitterionic polymers such as phosphoryl cholines (PC) attracted a lot of attention once the discovery of zwitterionic lipid phosphatidylcholines as the major component of the external layer of erythrocytes known to be non-thrombogenic. Thus, they are considered as antifouling candidates, possessing a native bio- and haemocompatibility [1-4]. Furthermore, over the years, PC-based substrates or coatings have been shown to possess superior antifouling properties, high resistance to biofilm formation and bacterial adhesion, making them promising candidates for biomedical applications such as hernia or cardiovascular implants, biosensing, contact lenses and many other. In the present study we grafted PC moieties on gelatin subsequently used as a coating for polypropylene (PP) mesh intended for hernia implants.

METHODS: Briefly, gelatin was modified to methacrylated gelatin using known protocols and PC moieties were subsequently introduced using 2-methacryloyloxyethyl

phosphorylcholine from Sigma Aldrich. A 1mg/mL solution of thus freeze-dried derivative was further used to obtain PC-tethered coatings on synthetic films and their antifouling properties were investigated against BSA and IgG model fluorescent labelled proteins by fluorescence microscopy. Basic characterization methods such as FTIR, UV-VIS, SCA, etc, were applied in the study.

RESULTS: Thus obtained PC-polymer derivatives were used as potential antifouling coating on synthetic polymer meshes with known hydrophobic. Significant reduction in BSA and IgG protein adsorption was seen in the case of PP meshes coated with PC-based derivatives compared with pristine films (without a coating). In addition, the influence of presence of a plasma treatment before coating application was seen, where plasma treated surfaces presented a more homogeneous coating and therefore an increase in antifouling behavior.

DISCUSSION & CONCLUSIONS: Antifouling properties were shown to be enabled by PC-tethered natural-based polymer coatings, which opens new opportunities in using such derivatives as alternatives for PEG-based coatings and/or in biomedical applications.

ACKNOWLEDGEMENTS: This work was supported by a grant of the Ministry of Research, Innovation and Digitization, CNCS/CCCDI – UEFISCDI, project number PD141/2020, within PNCDI III. Authors would like to thank both Politehnica University and Cantacuzino Institute for their support.

REFERENCES: [1] Engler et al., *Macromolecules*, **2015**, v. 48(6), p. 1673; [2] Hatakeyama et al., *Biol Pharm Bull*, **2013**, v. 36(6), p. 892; [3] Knop et al., *Angew Chem Int Ed Engl*, **2010**, v. 49(36), p. 6288; [4] Lewis, *Colloids and Surfaces B: Biointerfaces*, **2000**, v. 18(3), p. 261.

Synthesis of Octacalcium Phosphate

R. Choudhary^{1,2}, J. Locs^{1,2}

¹*Rudolfs Cimdins Riga Biomaterials Innovations and Development Centre of RTU, Faculty of Materials Science and Applied Chemistry, Institute of General Chemical Engineering, Riga Technical University, Riga, Latvia,* ²*Baltic Biomaterials Centre of Excellence, Headquarters at Riga Technical University, Riga, Latvia*

INTRODUCTION: Octacalcium phosphate (OCP, $\text{Ca}_8\text{H}_2(\text{PO}_4)_65\text{H}_2\text{O}$) has been indicated as a precursor of biological apatite crystals in the bone, as well as tooth dentin and enamel. In terms of collagen formation, the osteoconductivity of OCP is more than hydroxyapatite and tri-calcium phosphate [1]. The synthesis of OCP is highly influenced by molarity, pH, temperature, and order of reagent addition and stirring rate. A slight alteration in reaction parameters often leads to the formation of undesirable phases [2]. As a result, the synthesis of OCP is found to be very challenging and time-consuming.

METHODS: OCP was synthesized by the precipitation method. Phosphate buffer (250 mL) was added directly into the calcium acetate (250 mL) solution. The Ca/P ratio used in this experiment was 1.33. The pH of the reaction mixture was maintained at 6 by adding the required amount of sodium hydroxide. The reaction was carried out at 60 °C, with a stirring rate of 520 rpm for four hours. After the completion of the reaction, the precipitate was centrifuged three times using distilled water, followed by freeze-drying and lyophilization. The phase confirmation of OCP was analyzed by XRD. The surface morphology of the sample was characterized by SEM.

RESULTS:

Fig. 1 shows the XRD pattern of the synthesized sample. The characteristic peaks observed in the XRD pattern matched with the standard octacalcium phosphate pattern [ICDD card no. 00.026.1056].

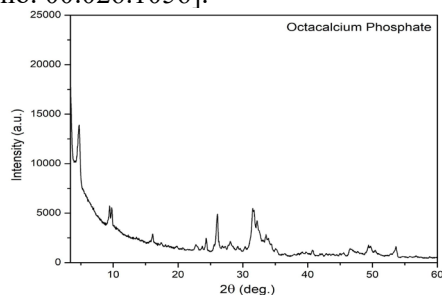


Fig. 1: XRD pattern of prepared octacalcium phosphate.

It was also found that the sample appeared as low crystalline OCP. The surface morphology of OCP was found to have flake-like structures distributed throughout the surface (fig. 2). Similar morphology was found in the previously published articles.

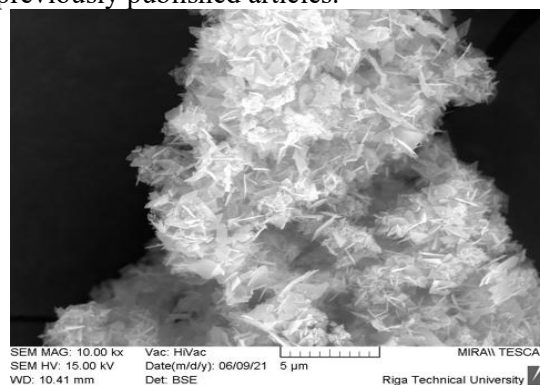


Fig. 2: SEM micrograph of prepared octacalcium phosphate.

DISCUSSION & CONCLUSIONS: The reaction conditions required for the preparation of OCP were optimized. This study confirms the synthesis of OCP within 4 hours.

ACKNOWLEDGEMENTS: The authors gratefully acknowledge European Union's Horizon 2020 research and innovation programme under grant agreement No. 857287.

REFERENCES: [1] O. Suzuki et al., Dent. Mater. J., **2020**, v. 39, p. 187; [2] L.C. Chow, E.D. Eanes (eds): Octacalcium Phosphate. Monographs in Oral Science. Basel, Karger, **2001**, v. 18, p. 94.

Hemostatic Antibacterial Wound Dressing for Accelerated Blood Stop

M. Sedlář¹, K. Kacvinská¹, R. Dvořák², T. Sopuch³, L. Vojtová¹

¹CEITEC - Central European Institute of Technology, Brno University of Technology, Brno, CZ, ²Hemcon Medical Technologies CZ s.r.o., Za Mlýnem, Tišnov, CZ, ³Holzbecher, spol. s.r.o barevna a bělidlo Zlích, Česká Skalice – Zlích, CZ

INTRODUCTION: The bleeding is one of the most commonly occurring injuries. From minor scratches to lacerations and even combat wounds. These wounds could be very painful, be a place where infection enters a body and might lower a person's overall condition [1]. The answer to deal with these problems could be a new hemostatic antibacterial wound dressing that will accelerate hemostasis and have antibacterial properties. Our vision and the primary goal of this work was to develop, manufacture, and characterise the physical, chemical, and hemostatic properties *in vitro* of a hemostatic wound dressing from a mixture based on oxidised cellulose, chitosan, and carboxymethylcellulose. Using a combination of these materials should give us improved properties of the final product. Mixing substances in the right composition and ratios will allow us to take full advantage of the material properties synergy.

METHODS: Dressing based on chitosan, oxidised cellulose and carboxymethylcellulose sodium salt were prepared in the form of sponges by the freeze-drying process. Prepared foams were characterised by infrared spectroscopy (ATR-FTIR) to confirm chemical composition. SEM images were obtained for morphology information (the porosity, size, and shape of pores). The absorption capacity of simulated fluids was determined according to ČSN EN 13726-1. For hemostatic properties, different *in vitro* methods were used, e.g., blood clotting assays, clotting time, and enzymatic test.

RESULTS: The materials work as great hemostatic agents on their own, but when combined, the results for absorption capacity, clotting time and other results showed an interesting increase in desirable properties.



Fig. 1. Hemostatic wound dressing after absorption capacity testing.

DISCUSSION & CONCLUSIONS: The results showed a great synergy of used materials. The lyophilised sponges based on chitosan, carboxymethylcellulose and oxidised cellulose have very promising results for the absorption capacity and for the conducted *in vitro* hemostatic testing with porcine blood. These results show that using a mixture of commonly used hemostatic biomaterials could bring some improved results and the final product might have added value.

ACKNOWLEDGEMENTS: This work was supported by the project Quality Internal Grants of BUT (KInG BUT), Reg. No. CZ.02.2.69 / 0.0 / 0.0 / 19_073 / 0016948, which is financed from the OP RDE. CzechNanoLab project LM2018110 funded by MEYS CR is gratefully acknowledged for the financial support of the measurements at CEITEC Nano Research Infrastructure.

REFERENCES:

[1] Y. Yang et al., *Bioactive Materials*, 2022, v. 8. doi:10.1016/j.bioactmat.2021.06.014

Spatiotemporally Modulated Magnetic Fields Induce Activation of Voltage-Gated Sodium Channels in Skeletal Muscle Cells

M. Rubio Ayala¹, V. Zablotskii², A. Dejneka², Th. Simmet¹, T. Syrovets¹

¹*Institute of Pharmacology of Natural Products & Clinical Pharmacology, Ulm University, Ulm, Germany,* ²*Institute of Physics Academy of Sciences of the Czech Republic, Prague, Czech Republic*

INTRODUCTION: Electric and magnetic fields (EMFs) produced by biological tissues are mainly defined by the cell-membrane potential, which also controls different cell functions. The membrane potential is particularly important in muscles, where its small variations control muscle contraction enabling moving, walking, holding objects, and heart beating. Hence, it might be possible to manipulate cell metabolism and muscle contraction by application of suitable external EMFs. In this regard, magnetic fields have an important advantage over electrical fields as they are much less attenuated by tissues, penetrate into deeper tissue layers, and can therefore be used to affect biochemical processes linked to changes in signalling pathways and cell biological events.

METHODS & RESULTS: We used complex spatiotemporal magnetic fields of several mT to control intracellular signalling in skeletal muscle cells. By changing amplitude, inversion time, and rotation frequency of the alternating magnetic fields, we induced transient depolarization of cellular membranes, which resulted in activation of voltage-gated sodium channels (VGSC) and temporal elevation of intracellular Na^+ levels (Na^+_i). Increased Na^+_i induced activation of ryanodine receptors and cytosolic calcium increase (Ca^{2+}_i). Elevated levels of Ca^{2+}_i triggered formation of filamentous actin, which forms thin filaments critical for muscle contraction. Actin polymerization was VGSC- and ryanodine receptor-dependent and was abolished in the presence of corresponding inhibitors. The ion fluxes occurred only, when the field was applied, and they returned to baseline after the field was switched off. A 30-sec-activation-cycle could be repeated without any loss of signal intensity. By contrast, static magnetic fields of the same strength exhibited no effect on the Ca^{2+}_i levels in myotubes. A modeling study elucidated the key mechanism of the membrane depolarization due to the Eddy current, which produces a local membrane

potential variation of 8 mV. This alteration is capable of triggering activation of VGSC, sodium flux, and a cascade of intracellular biochemical reactions resulting in ryanodine activation and actin polymerization, effects similar to those induced by the VGSC-opener veratridine.

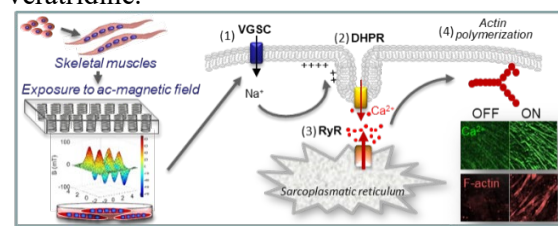


Fig. 1: Mechanism of action of spatiotemporally modulated magnetic fields.

DISCUSSION & CONCLUSIONS: We demonstrate that VGSC serve as the major effectors of the alt-magnetic field in skeletal muscles cells. Furthermore, we show that adjusting the parameters of the alt-magnetic field (field amplitude, inversion, and/or rotation time) one can tune the cytosolic level of Ca^{2+}_i and drive actin polymerization.

The elaborated model provides a universal framework encompassing current studies on Ca^{2+}_i signalling triggered by alternating magnetic fields. Mathematical modelling suggests a role for the alternating magnetic field-induced Eddy current, which mediates a local change in the membrane potential triggering the activation of VGSC.

This study opens intriguing perspectives for engineering new devices delivering magnetic fields permitting remote control for clinical applications to treat a number of myopathies.

ACKNOWLEDGEMENTS: This work was supported by the Volkswagen Foundation, Project ID 8839.

REFERENCES: [1] M. Rubio Ayala et al., *Biomaterials*, **2018**, v. 163, p. 174.

Fracture Resistance of Endodontically Treated Molars, Restored with Different Material Overlays and Endocrowns. A Pilot Study

S. Miļuna¹, B. Sprinģe¹, E. Papia²

¹Rīga Stradiņš university, Department of Prosthetic Dentistry, Riga, Latvia, ²Malmö University, Faculty of Odontology, Department of Materials Science and Technology, Malmö, Sweden

INTRODUCTION: To restore an endodontically treated molar tooth with indirect restoration that both preserves and protects the residual tooth structure is challenging. Besides the conventional crown, which demands invasive tooth preparation, overlay and endocrown is a less invasive approach to cover weakened tooth cusps, avoiding catastrophic tooth fracture. Tooth preparation for an overlay is more complex, eventually ensuring even thickness of restorative material to cover all tooth cusps and a composite build up in the middle. Meanwhile tooth preparation for an endocrown is less complex, ensuring one monolithic restoration to replace missing tooth structure (without composite build up) and cover all tooth cusps. The aim of this study was to evaluate the fracture resistance and fracture patterns of endodontically treated molar teeth, restored with ceramic and composite overlays and endocrowns.

METHODS: This prospective cross-sectional in vitro study involved 55 extracted molars, collected from the Clinic of Oral and Maxillofacial Surgery, at the Institute of Stomatology, Rīga Stradiņš University. All patients agreed to participate in the study, with consent for collecting biological material. Permission for this research was obtained from the Ethics Commission of Rīga Stradiņš University (An Ethics approval Nr. 22-2/94/2021). Extracted molars were disinfected and stored in distilled water at room temperature. Teeth were evaluated according to the inclusion criteria: extracted maxillary and mandibular molar teeth with remaining all intact roots, crown part with intact buccal and palatal (lingual) walls (occlusal/cuspal defect until 1,5 mm in depth acceptable), intact marginal ridges or proximal defects at least 1.0 mm above the cemento-enamel junction, no visible cracks. Fillings and/or caries were removed, and further evaluation was obtained based on the secondary inclusion criteria. 40 extracted molars met the criteria for further research. Endodontic root canal treatment was

performed for each tooth based on the endodontic treatment protocol. Teeth were divided according to 4 different restoration protocols: composite core build up with pressed Lithium Disilicate overlay (n=10); composite core build up with milled composite overlay (n=10); pressed Lithium Disilicate endocrown without composite build up (n=10); milled composite endocrown without composite build up (n=10). For overlay and endocrown restorations teeth were prepared according to criteria based on Veneziani, 2017. Composite build up was made with Optibond FL and G-aenial PA2 packable composite material. All teeth were scanned with the 3Shape Trios dental scanner. Dental technical laboratory, using CAD CAM technology, digitally planned the shapes for the desired restorations according to the plan and covering the occlusal surface equally ~ 1.5 mm in thickness. All restorations were cemented with Panavia V5, Kuraray, Noritake, according to adhesive cementation protocol. Teeth were sent to Malmö University, Sweden, for thermocycling loading (10000 cycles, 5°-55° C) for 7 days, chewing simulator (0-50 N, 1.6 Hz, 600000 cycles in 10° slope) for 7 days, thermocycling loading (10000 cycles, 5°-55° C) for 7 days.

RESULTS: Average lithium disilicate overlay fracture load was 1749 N, for lithium disilicate endocrowns 1052 N, for composite endocrowns 1656 N.

DISCUSSION & CONCLUSIONS: Lithium disilicate overlays had the highest fracture resistance. The presence of composite build up is necessary for developing fracture resistance.

ACKNOWLEDGEMENTS: We thank dental technicians from the Institute of Stomatology, Rīga Stradiņš university for collaboration.

REFERENCES: [1] M. Veneziani, The international journal of esthetic dentistry, **2017**, v. 12; [2] F. Ferraris, Int J Esthet Dent., **2017**, v. 12(4), p. 482.

Influence of Extracts from Damaged Murine Bones on MG63 and NIH3T3 Cell Proliferation Rate and Metabolic Activity

A. Metlova^{1,2}, I. Cesnokova^{1,2}, A. Sizovs^{1,2}

¹Latvian Institute of Organic Synthesis, Riga, Latvia, ²Baltic Biomaterials Centre of Excellence, Headquarters at Riga Technical University, Riga, Latvia

INTRODUCTION: Bone fracture site is an environment enriched with signaling molecules which orchestrate fracture healing process. The communication between cells in an organism has an important role in the recovery process of the fractured bones [1,2]. Signaling molecules coordinate cell migration, differentiation, and proliferation at the fracture site, which promotes for the callus formation and a mature bone formation [3]. Extracts from of the damaged murine bones containing released signaling molecules were applied to model cell lines to study their proliferative and metabolic responses.

METHODS: Bones were harvested from 6 euthanized mice and used immediately. Femurs and tibias were separated and cleaned from muscles and ligaments. Bones from each animal were separated into two groups: fractured, obtained by making several cuts with scissors; intact, used as is. Femurs and tibias, fractured or intact, were separately incubated in serum-free cell growth medium for 1 h. The resultant extracts were sterilized by 0.2 µm filtration. Bone extracts were diluted with 10% FBS and added to cultured human osteoblast-like cells (MG63) and cultured mouse fibroblasts (NIH3T3). Semi-automated cell counting and MTT assays were performed after 1, 3 and 7 days of incubation at 37 °C.

RESULTS: Within seven days tibia extracts increased the number of MG63 cells by 34 ± 10% ($p < 0.0001$) per well, fractured tibia extracts increased the number of cells by 38 ± 10% ($p < 0.0001$), whereas femur extracts – by 13 ± 11% ($p < 0.05$) (Fig.1). Damaged murine bone extracts did not have a significant impact on cell metabolic activity during seven days. Extracts from femurs and fractured femurs increased the number of NIH3T3 cells by 74±30% ($p < 0.01$) and by 39±27% ($p < 0.05$) accordingly after 1 day in comparison with the control group. After 1-day tibia extract increased metabolic activity of NIH3T3 cells by 74±28% ($p < 0.05$), while fractured tibia extracts

increased it by 96±26% ($p < 0.01$) in comparison with the control group.

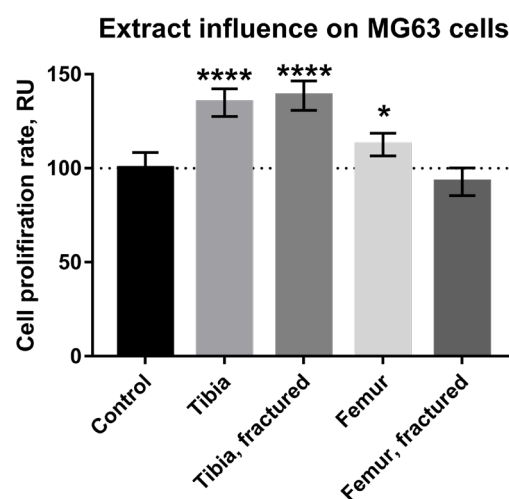


Fig. 1. Proliferation rate of MG-63 osteoblast-like cells was influenced by the extract from murine bones. $n=5$, ANOVA, followed by Dunnet's test; ****($p < 0.0001$), *($p < 0.05$).

DISCUSSION & CONCLUSIONS: Extracts from damaged bones positively affected proliferation rate of MG63 cells, especially the extracts from tibia (Fig.1). Metabolic activity of osteoblasts, however, was not affected. Extracts of both intact and fractured femurs enhanced proliferation rate of fibroblasts after 1 day of incubation. At the same time, only extracts of tibia boosted fibroblast metabolic activity after 1 day.

ACKNOWLEDGEMENTS: European Union's Horizon 2020 research and innovation programme under the grant agreement No 857287.

REFERENCES: [1] F. Loi et al., Bone, **2016**, v. 86, p. 119; [2] K.D. Hankenson et al., Adv Drug Deliv Rev, **2015**, v. 94, p. 3; [3] A.R. Armiento et al., Adv Funct Mater, **2020**, v. 30(44), p. 1.

Amorphous Calcium Phosphate Ceramics with Controlled Porosity

K. Rubenis^{1,2}, S. Zemjane^{1,2}, J. Locs^{1,2}, D. Loca^{1,2}

¹Rudolfs Cimdins Riga Biomaterials Innovations and Development Centre of RTU, Institute of General Chemical Engineering, Faculty of Materials Science and Applied Chemistry, Riga Technical University, Riga, Latvia, ²Baltic Biomaterials Centre of Excellence, Headquarters at Riga Technical University, Riga, Latvia

INTRODUCTION: Amorphous calcium phosphate (ACP) is a metastable calcium phosphate phase. It has excellent biocompatibility and better resorbability than hydroxyapatite, and therefore it is used in different biomaterials. However, currently, its use is restricted to the form of powder or coating. Due to the metastability, it is challenging to produce ACP in a bulk form that has limited its potential applications. Recently, we showed that ACP can be sintered to near-full density by uniaxial compaction at room temperature. However, for practical applications, calcium phosphate ceramics with controlled porosity is needed. In the present study, we investigated the possibility to produce porous amorphous calcium phosphate ceramics samples by using space holder technique to introduce porosity into ACP ceramics.

METHODS: ACP was synthesized by the dissolution-precipitation method [1]. The synthesized ACP was mixed with a space holder (multiple space holders were investigated, volume percentage of space holder up to 70 %). Then, the mixture was transferred to a pressing die and uniaxial pressure up to 1500 MPa was applied to it. The space holder from the obtained samples was removed by leaching in an appropriate solvent. Afterwards, the samples were characterized by X-ray diffraction, Fourier-transform infrared spectroscopy and scanning electron microscopy. Their bioactivity was evaluated by immersion into phosphate buffered saline solution.

RESULTS: The samples with a space holder content up to 60% by volume did not disintegrate during the leaching process. XRD and FTIR confirmed that amorphous calcium phosphate phase was retained after the compaction and leaching process, however, changes were induced in their local structure. Pronounced apatite layer formation on the surface of the amorphous calcium phosphate ceramics samples were observed already at the first days after immersion in the PBS solution.

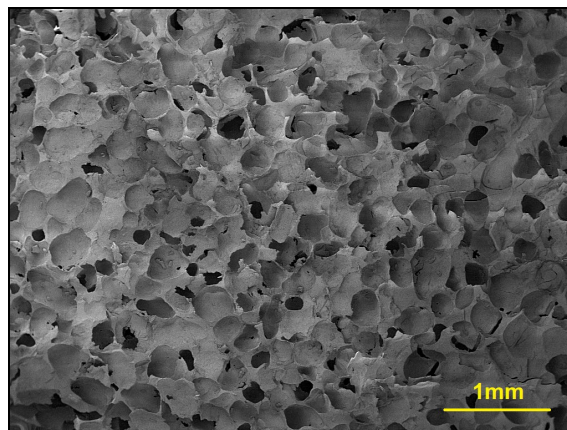


Fig.1. The fracture surface morphology of the ACP sample with 60% porosity (by volume).

DISCUSSION & CONCLUSIONS: The results suggest that space holder method can be used to produce ACP ceramics with controlled porosity if uniaxial compaction is used for sintering of ACP.

ACKNOWLEDGEMENTS: The authors acknowledge financial support from the Baltic Research Programme project No. EEA-RESEARCH-85 “Waste-to-resource: eggshells as a source for next generation biomaterials for bone regeneration (EGGSHELL)” under the EEA Grant of Iceland, Liechtenstein and Norway No. EEZ/BPP/VIAA/2021/1.

REFERENCES: [1] J. Vecstaudza et al., *J. Alloys Compd.*, **2017**, v. 700, p. 215; [2] K. Rubenis et al., *J. Eur. Ceram. Soc.*, **2021**, v. 41, p. 912.

Pros and Cons of Cannabidiol Encapsulation in Liposomes

N.L. Zukule^{1,2}, M. Skrinda-Melne^{1,2}, M. Brante¹, A. Grava^{1,2}, A. Dubnika^{1,2}

¹*RTU Rudolfs Cimdins Riga Biomaterials Innovation and Development Centre, Faculty of Materials Science and Applied Chemistry, Riga Technical University,* ²*Baltic Biomaterials Centre of Excellence, Headquarters at Riga Technical University, Riga, Latvia*

INTRODUCTION: Liposomes are spherical drug vehicles. They are mainly composed of phospholipids, which occur in cell membrane's structure, making liposomes highly biocompatible with the body. Studies have shown that Cannabidiol (CBD) has a wide range of medical applications, including pain-relief, anti-inflammatory, anticonvulsive and cancer cell antiproliferative effect [2], but it is highly unstable. Incorporation into liposomes provides more efficient absorption of lipophilic CBD into body fluids. In this study we are looking at the pros and cons of the CBD encapsulation [3,4].

METHODS: Blank and CBD containing liposomes were synthesized using the freeze-thawing method, shortly: liposomes were composed of 1,2-distearoyl-sn-glycero-3-phosphocholine (DSPC) and Cholesterol in molar ratio 2/1, lipids were dissolved in absolute ethanol. For CBD liposomes, CBD was dissolved along with the lipids. Ethanol was evaporated using a rotary evaporator and afterwards deionized water was gradually added to the samples. 3 freeze-thaw cycles were performed. Stability of CBD in liposomes in water solution was evaluated for 4, 7, 14 and 21 days. The structure and morphology for blank and drug loaded liposomes was assessed with FT-IR and SEM. Cytotoxicity was evaluated on 3T3 mouse fibroblasts. Lyophilized liposome powder was rehydrated in full cell medium. After preparing 100 μM stock solution of both liposomes, it was diluted to 0.5, 1, 2, 3, 5, 7, 10, 12 μM . 200 μL of each solution was added to cells for 24h and 48h. The results were evaluated with neutral red (NR) test. Untreated cells were used as control.

RESULTS: Liposomes had high stability of CBD after 4 days – 61.77%, after 7 days it decreased to 41.13%, and 12.09% after 21 days. But the results contradicted with other studies [5-7], stating that liposomes are stable up to 3 months, as CBD in the water without liposomal system showed higher stability (80.33% in 7 days). In the obtained SEM images, spherical structure liposomes and several crystals can be

seen, which formed during lyophilization. In the FT-IR spectrum it is possible to see both the lipid peaks and the signals characteristic of CBD. The obtained cytotoxicity results show that both blank and CBD loaded liposomes have cell viability is above 70% after 48h. Liposomes containing CBD have cell viability from 90-105%, on the other hand blank liposomes have cell viability up to 117% after 48h time point.

DISCUSSION & CONCLUSIONS: CBD increases cell proliferation after 48h in concentration from 1 μM to 3 μM . Raval et al has concluded that CBD in concentrations from 0.01 μM to 2 μM raises transforming growth factor β (TGF- β) concentration. On the other hand, the stability studies in water showed that CBD can be recovered in higher amounts without the liposomal encapsulation. Further studies are needed to set the line between the stability and bioavailability of the CBD in liposomal systems.

ACKNOWLEDGEMENTS: This research has received funding from the the M-era.Net 2 project INJECT-BIO under agreement No. ES RTD/2020/14 and European Union's Horizon 2020 research and innovation programme under the grant agreement No 857287.

REFERENCES: [1] Large et al., *Adv. Drug Deliv. Rev.*, **2021**, v. 176, 113851; [2] Shohami et al., *J. Basic Clin. Physiol. Pharmacol.*, **2016**, v. 27(3), p. 175; [3] Koch et al., *Int. J. Pharm.*, **2020**, v. 589, 119812; [4] Bruni et al., *Molecules*, **2018**, v. 23(10); [5] Sannikova et al., <https://rb.gy/uzaarg/>; [6] Onaivi et al., *Nanomedicine*, **2020**, v. 15(21), p. 2023; [7] Verrico et al., *Pain*, 2020, v. 161(9), p. 2191.

Systemic Metabolism Changes During Bone Healing

A. Vaska^{1,2}, J. Fan^{1,2}, A. Sizovs^{2,3}, J. Locs^{1,2}, K. Klavins^{1,2}

¹Rudolfs Cimdins Riga Biomaterials Innovations and Development Centre, Riga Technical University, Riga, Latvia, ²Baltic Biomaterials Centre of Excellence, Headquarters at Riga Technical University, Riga, Latvia, ³Latvian Institute of Organic Synthesis, Riga, Latvia

INTRODUCTION: In recent years, the biomaterials for bone regeneration ability to modulate the local immune environment for favorable treatment outcomes have attracted significant research interest. The usage of bioactive metabolites has emerged as one of the most novel and potent approaches. The incorporation of metabolites with immune regulatory properties seems a desirable option for biomaterials as it would ensure a site-specific delivery system and allow modulation of the microenvironment. In this work, we characterized systemic metabolism changes during bone healing to pinpoint the perturbed metabolic processes and identify metabolites with potential immunomodulatory properties.

METHODS: Here, rat calvarial critical-size defects were used to characterize the metabolite changes in blood during bone healing. The trephine techniques were used to create a 5 mm diameter circular defect. For one group (n=6) defect site was left untreated. For the second group (n=5), the removed calvaria was split into 4 parts and placed back in the defect site. The blood samples were taken 1, 2, and 3 days after surgery. Metabolites were extracted following a methanol-based extraction protocol. Targeted quantitative metabolite analysis was performed using HILIC-based separation combined with mass spectrometric detection employing Thermo Orbitrap QExactive mass spectrometer.

RESULTS: The quantitative data for 33 metabolites, including amino acids, acylcarnitines, and biogenic amines, were obtained. The blood concentration of most of the amino acids was significantly decreased after surgery. However, acylcarnitines levels increased. Among the influenced metabolites, glutamine showed the highest statistical significance (Fig. 1).

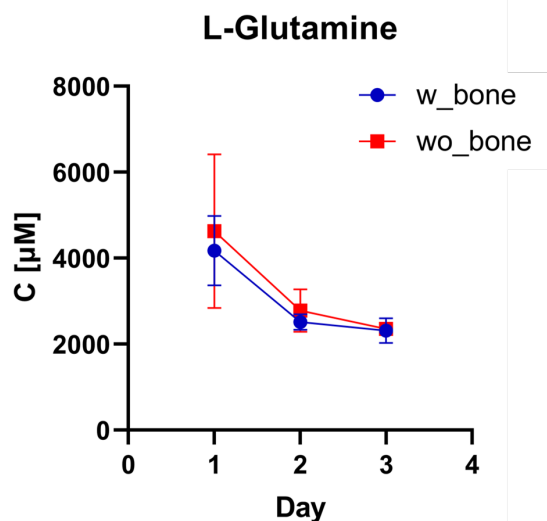


Fig. 1: Concentration of glutamine in the rat blood samples after induction of calvarial critical-size defect.

DISCUSSION & CONCLUSIONS: Changes in blood sample metabolite concentration provided evidence of organism-level metabolic adaptation to facilitate bone healing. Notably, the glutamine levels were significantly decreased after bone defect. Glutamine plays an essential role in several biological processes, including proliferation and lineage allocation in skeletal stem cells, protein synthesis, and tissue healing. We hypothesize that the glutamine level in the blood is depleted to ensure the nitrogen, amino acids, and energy necessary to regenerate lost tissue.

ACKNOWLEDGEMENTS: The authors acknowledge financial support from European Union's Horizon 2020 research and innovation programme under the Marie Skłodowska-Curie grant agreement No. 898858 and European Union's Horizon 2020 research and innovation programme under the grant agreement No. 857287.